LUND UNIVERSITY

Optimising External Beam Radiotherapy for Prostate Cancer. Advances in Treatment Planning

Jóhannesson, Vilberg

2024

Document Version:
Publisher's PDF, also known as Version of record

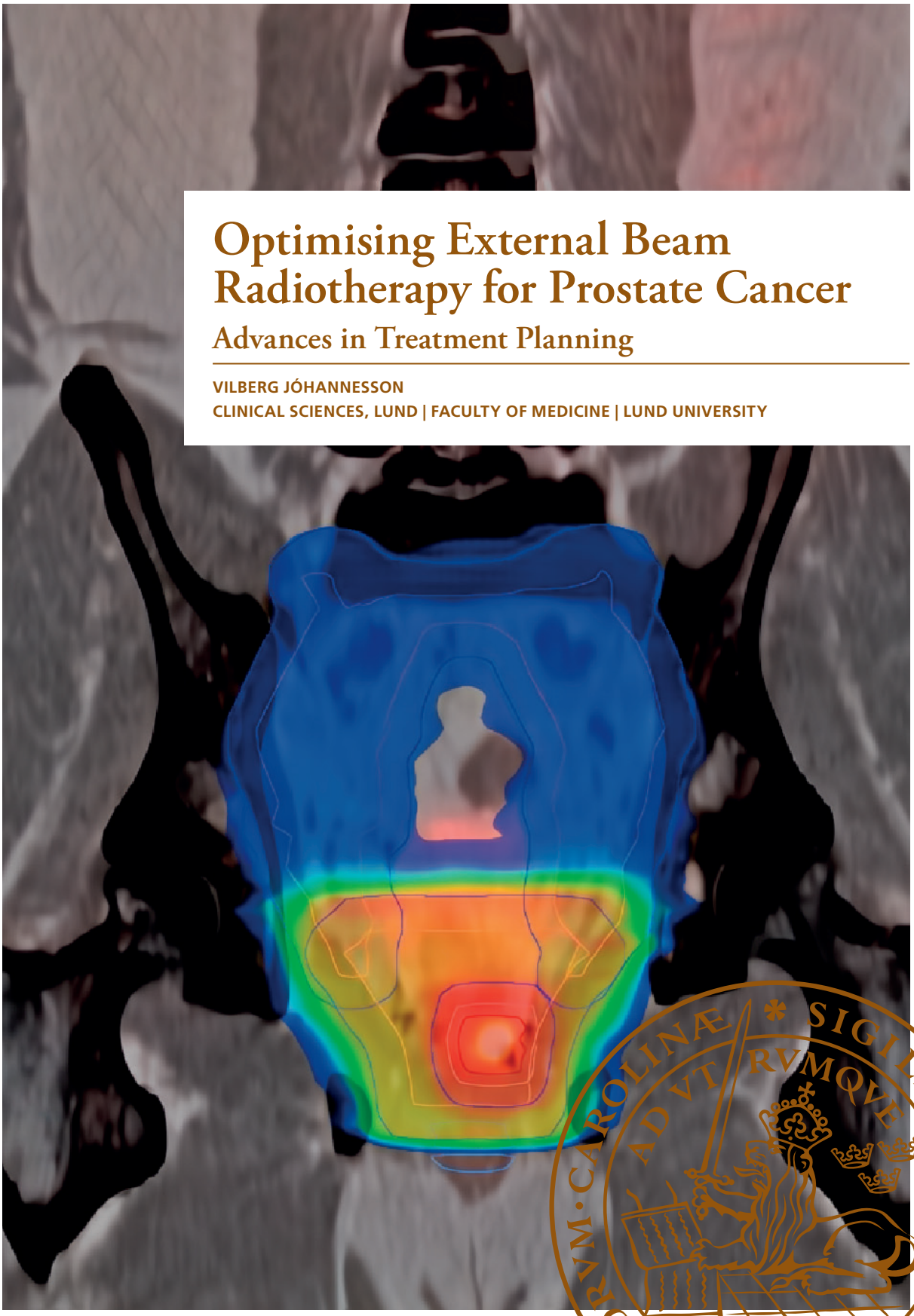

Optimising External Beam Radiotherapy for Prostate Cancer

Advances in Treatment Planning

VILBERG JÓHANNESSON
CLINICAL SCIENCES, LUND | FACULTY OF MEDICINE | LUND UNIVERSITY

VILBERG JÓHANNESSON is a Radiologic Technologist with a B.Sc. from the Technical College of Iceland and is a licensed radiology/oncology nurse that currently works as a medical dosimetrist at Skåne University Hospital in Lund, Sweden. He has a particular interest in radiotherapy treatment planning, inspired by Zheng et al. [120], *"Treatment planning, the design of radiotherapy for each individual case, is at the heart of radiotherapy and is thought of as both a science and an art."* This thesis contributes to the development and improvement of radiotherapy treatment planning methods for prostate cancer patients.

Printed by Media-Tryck, Lund 2024 NORDIC SWAN ECOLABEL 3041 0903

LUND UNIVERSITY

FACULTY OF MEDICINE

Department of Clinical Sciences, Lund

Lund University, Faculty of Medicine
Doctoral Dissertation Series 2024:50
ISBN 978-91-8021-543-5
ISSN 1652-8220

Optimising External Beam Radiotherapy for Prostate Cancer

Optimising External Beam Radiotherapy for Prostate Cancer

Advances in Treatment Planning

Vilberg Jóhannesson

DOCTORAL DISSERTATION

by due permission of the Faculty of Medicine, Lund University, Sweden.
To be defended in the Torsten Landberg lecture hall, Radiotherapy building 3rd floor, Klinikgatan 5, Skåne University Hospital, Lund, on Friday, April 19th, 2024, at 9:00 am.

Faculty opponent
Associate Professor Niclas Pettersson,
Department of Medical Radiation Sciences, Institute of Clinical Sciences,
Sahlgrenska Academy, University of Gothenburg, Gothenburg, Sweden
Department of Medical Physics and Biomedical Engineering,
Sahlgrenska University Hospital, Gothenburg, Sweden

Organisation: LUND UNIVERSITY
Department of Clinical Sciences, Lund

Faculty of Medicine

Author(s): Vilberg Jóhannesson

Document name:
DOCTORAL DISSERTATION

Date of issue: 2024-04-19

Sponsoring organisation:

Title and subtitle: Optimising External Beam Radiotherapy for Prostate Cancer - Advances in Treatment Planning

Abstract:

Background

Radiotherapy (RT) is an effective treatment option for prostate cancer (PCa). The evolution of new treatment planning techniques, advanced imaging and accelerator design has enabled precise treatment delivery. Volumetric modulated arc therapy (VMAT) optimisation techniques achieve sharp dose gradients between the target and organs at risk (OAR) and have become the standard of care for PCa RT.

Aims

This project aimed to enhance and develop advanced radiation planning techniques for optimising VMAT for primary and recurrent prostate cancer. Additionally, we explored new adaptive radiation therapy approaches based on tumour biomarker response during the initial part of the RT for patients with recurrent disease (Papers I-II). The aims of the work in Paper III were to use image registration to compare the planned radiation doses with the estimated delivered doses. Additionally, the study aimed to examine their relation to side effects. Furthermore, we assessed the feasibility of using the simultaneous integrated boost (SIB) VMAT technique for planning ultra-hypofractionated (UHF) RT in patients with targets including both the prostate and seminal vesicles (SV) (Paper IV).

Methods

A new treatment-planning concept was developed, including corrections for fractionation effects ($EQD2_{\alpha/\beta=3}$-dose conversions) with the so-called plan-on-plan technique in a prospective phase II trial (PROPER 1). The study included patients with biochemical recurrence after radical prostatectomy (RP), and all patients received RT to the prostate bed. Patients who did not have a prostate-specific antigen (PSA) response according to the study protocol during the first five weeks of RT were to receive additional treatment to regional lymph nodes (Papers I-II). Cone-beam computed tomography (CBCT) imaging data from the PROPER 1 study was used to analyse estimated delivered radiation dose distributions, comparing them with initial plans (Paper III) and evaluating potential dose-volume associations with side effects. In Paper IV, treatment structures have been redefined for patients within the HYPO-RT-PC trial, and we have estimated the feasibility of SIB techniques to include SV in the target volume with UHF fractionation compared with conventional fractionation (CF).

Results

Paper I: An EQD2 fractionation correction of the plan-on-plan for non-responding patients in PROPER 1 improved target dose coverage.

Paper II: The three-year failure-free survival was 94% for responders and 68% for non-responders, which compared favourably to historical controls. The study treatment was well tolerated.

Paper III: We have observed small but statistically significant differences between the planned and estimated delivered doses to OARs. These differences indicate improved associations between estimated delivered dose distributions and side effects.

Paper IV: UHF RT, based on the HYPO-RT-PC trial fractionation schedule, with a SIB technique to the prostate and the base of the SV, can be planned with generally lower doses to OARs.

Conclusions

To our knowledge, PROPER 1 is the only study presented on biomarker-guided sequential VMAT radiotherapy using a fractionation-corrected adapted plan-on-plan technique in the pelvis. This new personalised treatment concept with intensified SRT based on PSA response demonstrated a high tumour control rate in both responders and non-responders. These results have laid the foundation for the prospective randomised trial, PROPER 2 (NCT04858880).

Applying a SIB technique for treating both the prostate and the base of the seminal vesicles with UHF RT (based on the HYPO-RT-PC fractionation schedule) resulted in lower EQD2-corrected doses to organs at risk compared to conventionally fractionated radiotherapy delivered with sequential boost technique.

Key words:

Classification system and/or index terms (if any)

Supplementary bibliographical information

Language: English

ISSN and key title: 1652-8220

ISBN: 978-91-8021-543-5

Recipient's notes Number of pages: 82

Price

Security classification

Signature

Date 2024-03-07

Optimising External Beam Radiotherapy for Prostate Cancer

Advances in Treatment Planning

Vilberg Jóhannesson

LUND
UNIVERSITY

Cover: A coronal CT slice and PSMA-PET positive local recurrence with summed dose distributions in colour wash for a patient in the PROPER 1 study.

Cover by Vilberg Jóhannesson

Faculty of Medicine

Department of Clinical Sciences, Lund

ISBN 978-91-8021-543-5

ISSN 1652-8220

Printed in Sweden by Media-Tryck, Lund University, Lund 2024

To my cherished parents

"I don´t know where
I´m going from here,
but I promise it won´t
be boring"

David Bowie

Table of Contents

Abstract

Background

Radiotherapy (RT) is an effective treatment option for prostate cancer (PCa). The evolution of new treatment planning techniques, advanced imaging and accelerator design has enabled precise treatment delivery. Volumetric modulated arc therapy (VMAT) optimisation techniques achieve sharp dose gradients between the target and organs at risk (OAR) and have become the standard of care for PCa RT.

Aims

This project aimed to enhance and develop advanced radiation planning techniques for optimising VMAT for primary and recurrent prostate cancer. Additionally, we explored new adaptive radiation therapy approaches based on tumour biomarker response during the initial part of the RT for patients with recurrent disease (Papers I-II). The aims of the work in Paper III were to use image registration to compare the planned radiation doses with the estimated delivered doses. Additionally, the study aimed to examine their relation to side effects. Furthermore, we assessed the feasibility of using the simultaneous integrated boost (SIB) VMAT technique for planning ultra-hypofractionated (UHF) RT in patients with targets including both the prostate and seminal vesicles (SV) (Paper IV).

Methods

A new treatment-planning concept was developed, including corrections for fractionation effects ($EQD2_{\alpha/\beta=3}$-dose conversions) with the so-called plan-on-plan technique in a prospective phase II trial (PROPER 1). The study included patients with biochemical recurrence after radical prostatectomy (RP), and all patients received RT to the prostate bed. Patients who did not have a prostate-specific antigen (PSA) response according to the study protocol during the first five weeks of RT were to receive additional treatment to regional lymph nodes (Papers I-II). Cone-beam computed tomography (CBCT) imaging data from the PROPER 1 study was used to analyse estimated delivered radiation dose distributions, comparing them with initial plans (Paper III) and evaluating potential dose-volume associations with side effects. In Paper IV, treatment structures have been redefined for patients within the HYPO-RT-PC trial, and we have estimated the feasibility of SIB techniques to include SV in the target volume with UHF fractionation compared with conventional fractionation (CF).

Results

Paper I: An EQD2 fractionation correction of the plan-on-plan for non-responding patients in PROPER 1 improved target dose coverage.

Paper II: The three-year failure-free survival was 94% for responders and 68% for non-responders, which compared favourably to historical controls. The study treatment was well tolerated.

Paper III: We have observed small but statistically significant differences between the planned and estimated delivered doses to OARs. These differences indicate improved associations between estimated delivered dose distributions and side effects.

Paper IV: UHF RT, based on the HYPO-RT-PC trial fractionation schedule, with a SIB technique to the prostate and the base of the SV, can be planned with generally lower doses to OARs.

Conclusions

To our knowledge, PROPER 1 is the only study presented on biomarker-guided sequential VMAT radiotherapy using a fractionation-corrected adapted plan-on-plan technique in the pelvis. This new personalised treatment concept with intensified Salvage radiotherapy (SRT) based on PSA response demonstrated a high tumour control rate in both responders and non-responders. These results have laid the foundation for the prospective randomised trial, PROPER 2 (NCT04858880).

Applying a SIB technique for treating both the prostate and the base of the seminal vesicles with UHF RT (based on the HYPO-RT-PC fractionation schedule) resulted in lower EQD2-corrected doses to organs at risk compared to conventionally fractionated radiotherapy delivered with sequential boost technique.

Populärvetenskaplig sammanfattning

Prostatacancer är Sveriges vanligaste cancerform. Under 2022 var det 12000 män som fick diagnosen. En stor andel av dessa män får strålbehandling mot sin sjukdom. Genom åren har nya tekniker och teknologi gjort strålbehandling mer exakt och effektiv. En sådan utveckling är rotationsbehandling (VMAT, Volumetric Modulated Arc Therapy). Med denna teknik kan man koncentrera strålningen med hög noggrannhet till det cancerdrabbade området samtidigt som man skyddar frisk vävnad.

Huvudsyftet med denna avhandling var att utveckla och testa avancerade metoder för utformningen av strålbehandlingen för varje enskilt fall, kallad dosplanering, vid strålbehandling av prostatacancer med specifik fokus på VMAT tekniken. Det tvärvetenskapliga teamet bakom detta projekt som vi kallar PROPER, har utforskat nya sätt att anpassa strålbehandling baserat på hur tumören svarar på behandlingen, det vill säga individanpassa behandlingen. Vi har även jämfört de planerade stråldoserna med de faktiska doserna som levererats, och undersökt eventuella samband med de biverkningar som har rapporterats.

Ett nytt behandlingsplaneringskoncept för att kunna individanpassa strålbehandlingen, har utvecklats och förfinats med korrektioner för biologiska effekter från den strålbehandling som redan har givits. Vi har också observerat små men viktiga skillnader mellan den planerade stråldosen och den faktiska dosen som levererats till frisk vävnad i närheten av behandlingsområdet.

Sammanfattningsvis har denna avhandling visat att individanpassad strålbehandling, baserad på tumörsvar tillsammans med avancerad dosplanering, kan leda till bra tumörkontroll och sannolikt minskad risk för biverkningar. Resultaten från projektet har lagt grunden för en ny klinisk prövning benämnd PROPER 2.

Ultra-hypofraktionerad strålbehandling, det vill säga användning av höga stråldoser per behandlingstillfälle, men med reducerad totaldos, används i dag i allt större utsträckning mot prostatacancer. För vissa patienter vill man förutom prostata också inkludera sädesblåsorna i behandlingsområdet, men då ge en lägre stråldos till dessa än till själva prostatan. I denna avhandling utvärderades användningen av en teknik med vilken man kan ge olika stråldoser till olika områden i en och samma behandling, och i detta fall då just till prostatan och sädesblåsorna.

Resultatet visade att denna teknik kan planeras med generellt lägre doser till frisk vävnad i närheten av behandlingsområdet, jämfört med vår standardbehandling vid konventionellt fraktionerad strålbehandling.

List of Papers

I

Adaptive sequential plan-on-plan optimisation during prostate-specific antigen response guided radiotherapy of recurrent prostate cancer.
Johannesson V, Wieslander E, Nilsson P, Brun E, Bitzén U, Ahlgren G, Ohlsson T, Bäck S, Kjellén E, Gunnlaugsson A. Physics and Imaging in Radiation Oncology 2021; 18:5–10. https://doi.org/10.1016/j.phro.2021.03.001

II

A prospective phase II study of prostate-specific antigen-guided salvage radiotherapy and (68)Ga-PSMA-PET for biochemical relapse after radical prostatectomy – The PROPER 1 trial.
Gunnlaugsson A, **Johannesson V**, Wieslander E, Brun E, Bitzén U, Ståhl O, Bratt O, Ahlgren G, Ohlsson T, Kjellén E, Nilsson P.
Clinical and Translational Radiation Oncology 2022; 36:77-82.
https://doi.org/10.1016/j.ctro.2022.07.001

III

Dose-volume relationships of planned versus estimated delivered radiation doses to pelvic organs at risk and side effects in patients treated with salvage radiotherapy for recurrent prostate cancer.
Johannesson V, Gunnlaugsson A, Nilsson P, Brynolfsson P, Kjellén E, Wieslander E.
Technical Innovations & Patient Support in Radiation Oncology 2023; 29:100231.
https://doi.org/10.1016/j.tipsro.2023.100231

IV

Ultra-hypofractionated radiotherapy for prostate cancer including seminal vesicles in the target volume: a treatment-planning study based on the HYPO-RT-PC fractionation schedule.
Wieslander E, **Johannesson V**, Nilsson P, Kjellén E, *G*unnlaugsson A.
Manuscript

Author’s contribution to the papers

Paper I

I actively participated in the planning and development of the described radiation method, as well as in data acquisition, analysis, and interpretation. I also wrote the initial manuscript draft and participated in all stages of revisions and responses to journal reviews.

Paper II

I contributed to the planning of the PROPER 1 study by participating in protocol writing and actively engaging in the treatment planning of all 100 patients. I also contributed to analyses, manuscript writing, and the submission process.

Paper III

I participated in the study's planning, including defining the healthy tissues to be outlined. Based on 7-10 CBCT scans for each patient, I outlined organs at risk and generated several structures for analysis. I collected and analysed the data on side effects and quality of life. I wrote the initial manuscript draft and took responsibility for revisions and publication.

Paper IV

I participated in the overall study design. I outlined organs at risk for all 30 patients involved in the study. I created dose plans for all thirty patients, 14 plans for each, to enable analysis and comparison. I participated in data analysis led by the first author and contributed to manuscript writing.

Other related publications not included in this thesis

PSA decay during salvage radiotherapy for prostate cancer as a predictor of disease outcome – 5 year follow-up of a prospective observational study.
Gunnlaugsson A, Kjellén E, Bratt O, Ahlgren G, **Johannesson V**, Blom R, Nilsson P.
Clinical and Translational Radiation Oncology 2020; 23-28.
https://doi.org/10.1016/j.ctro.2020.05.008

Abbreviations

3D-CRT	Three-dimensional conformal radiotherapy
ADT	Androgen deprivation therapy
AS	Active surveillance
BCR	Biochemical recurrence
BED	Biologically effective dose
BEV	Beam's eye view
BT	Brachytherapy
CBCT	Cone-beam computed tomography
CF	Conventional fractionation
CT	Computed tomography
CTV	Clinical target volume
D	Dose (in Gray)
DIR	Deformable image registration
DVH	Dose-volume histogram
ED	Electron density
EPE	MRI detected extraprostatic extension
EQD2	Equivalent dose in 2Gy fractions
FFS	Failure-free survival
GI	Gastrointestinal
GTV	Gross tumour volume
GU	Genitourinary
Gy	Gray (unit of ionising radiation dose)
HDR-BT	High dose rate brachytherapy
IGRT	Image-guided radiotherapy
IMRT	Intensity-modulated radiation therapy
LINACs	Medical linear accelerators
LQ model	Linear-quadratic model
LDR-BT	Low dose rate brachytherapy

MHF	Moderate hypofractionation
MLC	Multi-leaf collimator
MRI	Magnetic resonance imaging
MU	Monitor units
MV	Megavoltage
NTO	Normal tissue objective
OAR	Organs at risk
PCa	Prostate cancer
PLNRT	Pelvic lymph node radiotherapy
PROM	Patient reported outcome measures
PSA	Prostate-specific antigen
PSMA-PET	Prostate-specific membrane antigen positron emission tomography
PTV	Planning target volume
RP	Radical prostatectomy
RT	Radiotherapy
SBRT	Stereotactic body radiation therapy
SRT	Salvage radiotherapy
SV	Seminal vesicles
SVI	Seminal vesicle tumour invasion
TPS	Treatment planning system
TRUS	Trans-rectal ultrasound
UHF	Ultra-hypofractionation
vDSC	volumetric Dice similarity coefficient
VMAT	Volumetric modulated arc therapy
α/β ratio	Alpha-beta ratio

Introduction

Radiotherapy is a highly effective treatment option for prostate cancer [1, 2]. Thanks to the development of new treatment planning techniques, advanced imaging, and accelerator design, RT can now be delivered with increased precision. VMAT optimisation techniques secure sharp dose gradients between the target and OARs and have become the standard of care for PCa RT.

Adaptation of an ongoing course of radiotherapy requires advanced treatment planning techniques. With the VMAT technique, dose distributions delivered previously can be taken into account during treatment plan optimisation using a "plan-on-plan" function in the treatment planning system (TPS), Varian Eclipse, after a change in treatment conditions [3].

Patients who experience biochemical recurrence (BCR) [4, 5] after a radical prostatectomy (RP) experience a rise in PSA levels. Salvage radiotherapy (SRT) to the prostate bed is the customary treatment in such cases. The recommended radiation dosage for SRT is 64-70 Gy, given at conventional fractionation (1.8-2.0 Gy per daily fraction) [6]. However, imaging methods frequently have failed to identify the site of recurrence at low PSA values. The decision to proceed with SRT is primarily based on the likelihood of local recurrence, which is predicted by tools such as the Stephenson nomogram [7]. The efficacy of pelvic lymph node radiotherapy (PLNRT) in SRT is currently unknown, but studies are underway [8]. Emerging imaging methods, such as ^{68}Ga-PSMA-PET-11 (PSMA-PET), have shown promise in detecting tumour recurrence at low PSA levels [9-12]. Combining PSA kinetics during SRT as a biomarker and PSMA-PET may enable more personalised treatment and identifying high-risk patients.

Pelvic radiotherapy (RT) presents challenges because of variations in organ volumes, which can be caused by factors such as bladder and bowel filling [13, 14]. Image-guided radiotherapy (IGRT) ensures adequate dose coverage, but daily organ volume and location variations pose challenges. Treatment planning guidelines have been based on static planned dose distributions and do not account for these daily variations. Differences in bladder volume between planned and actual volume during treatment could affect dose constraints [15]. Variations in dose metrics for the bladder and rectum were observed. In our third paper, we compare planned and estimated delivered dose distributions in pelvic OARs, using CBCT images to estimate the dose delivered throughout the entire treatment course.

The estimated dose delivered to organs at risk (OAR) and targets during the entire treatment course could be calculated based on CBCT images acquired at treatment. This can be accomplished by using deformable image registration (DIR) [16], where deformation fields based on registration between the planning CT and each CBCT are applied to either the dose calculated on each CBCT or the original dose distribution [17, 18]. The potential association between dose-volume metrics for these dose distributions and gastrointestinal (GI) and genitourinary (GU) side effects can then be studied. It has been suggested that the radiation dose to bladder sub-volumes, such as the urethra, the bladder wall, and the bladder trigone [19-25], has a stronger association with side effects than the dose to the whole organ [26].

Hypofractionation is commonly used in prostate cancer radiotherapy because of a proposed low α/β ratio [27]. Trials such as CHHiP [28], HYPRO [29], PROFIT [30], and RTOG 0415 [31] report comparable outcomes for moderate hypofractionation (MHF) (2.4-3.4 Gy per fraction) and conventional fractionation (CF) (1.8-2.0 Gy per fraction) for low to intermediate-risk localised prostate cancer. Ultra-hypofractionation (UHF) (>5 Gy per fraction) studies, like HYPO-RT-PC [32] and PACE-B [33], demonstrate efficacy and safety. UHF could be considered an alternative for localised prostate cancer. If there exists (risk of) tumour invasion in the seminal vesicles (SV), these are to be included in the target volume [34]. Including SV increases the irradiated volume, necessitating an exploration of its impact on organ doses and target volumes.

Research aims

The overall aim of this thesis was to develop and evaluate methods to accomplish a more individualised adaptive radiotherapy process by improving the treatment planning techniques for prostate cancer patients.

Paper I

Treatment adaptation based on tumour biomarker response during radiotherapy of prostate cancer could be used for both escalation and de-escalation of radiation doses and volumes. Executing an adaptation involving the extension of treatment volumes during radiation could, however, be restricted by the doses already delivered. This study aimed to develop a treatment planning method that addresses this challenge.

Paper II

In the PROPER 1 trial, a salvage radiotherapy study for prostate cancer, the primary objectives were to evaluate a new novel imaging method, ^{68}Ga-prostate-specific membrane antigen positron emission tomography (PSMA-PET) and to develop a novel adaptive treatment strategy involving sequential PLNRT and boost to PSMA-PET-positive lesions guided by PSA kinetics as a biomarker during SRT.

Paper III

The primary aim of this work was to compare planned and estimated delivered dose distributions in pelvic OARs for the patients enrolled in the PROPER 1 study. The secondary aim was to determine the potential association between dose-volume metrics for these dose distributions and gastrointestinal (GI) and genitourinary (GU) side effects.

Paper IV

The aim of the study was to assess the feasibility of implementing UHF simultaneous integrated boost (SIB) for prostate cancer RT, including SV, based on the HYPO-RT-PC fractionation schedule (7 fractions over 2.5 weeks).

Background

Development of external beam radiotherapy with high-energy photons

Radiation treatment equipment

During the late 19th century, the discovery of ionising radiation led to rapid adoption and use in clinical applications, both diagnostic and therapeutic. At that time, most tumours could not be cured with external RT without causing extensive damage to normal tissues, especially the skin, due to the limited penetration depth of the available radiation quality, often administered single high-dose fractions. During the early 20th century, the effects of fractionation were recognised, resulting in significant variations in treatment schedules. The ability of X-rays or γ-rays to penetrate biological tissue depends on the energy of the photons. Therefore, early radiotherapy was limited to devices that could only produce low-energy X-rays in the kilovoltage (kV) range. In the 1950s, medical linear accelerators (LINACs) producing Megavoltage (MV) X-rays were developed. Machines using cobalt-60 (^{60}Co) as a radiation source, emitting two photons with a mean energy of 1.25 MeV per decay, were also developed during the 1950s [35, 36]. MV and MeV X-rays penetrated deeper into the patient's body than kV X-rays and have a skin-saving effect. Cobalt-60 machines were widely used for radiotherapy through the late 20th century. However, their use has significantly declined with the advent of more advanced technologies such as LINACs. Modern LINACs are advanced and sophisticated devices with an energy typically ranging from 4 to 25 MV, featuring isocentric mounting and full rotation.

The multileaf collimator (MLC) was developed in the 1980s and gained more widespread clinical use during the 1990s, replacing the conventional cerrobend blocks mentioned above. The MLC is composed of two groups of slender tungsten leaves that can move separately in and out of the way of a radiotherapy beam, shaping it as needed. The use of a multileaf collimator enhances the precision and efficiency of radiation therapy, while also decreasing the duration of each treatment session, potentially allowing for more patients to be treated in a single day.

Intensity-modulated radiation therapy

Anders Brahme, a Swedish physicist, introduced the idea of rotational therapy in an article in 1982 [37] and laid the groundwork for Intensity-modulated radiation therapy (IMRT) in 1988 [38]. IMRT systems were initially introduced in the clinic in the early 1990s. They can be classified into two types: cone beam technology, delivered with a regular linear accelerator device, and fan beam technology, delivered with a helical tomotherapy device. 1994, the first IMRT treatment was reported using fan beam technology [39]. 1995, the first treatment using cone beam technology was presented [40]. IMRT was not commonly used in clinical practice until the early 2000s. The development of IMRT is considered to be the most successful advancement in radiation oncology since the introduction of CT into treatment planning.

In 2007, a new technique for IMRT called Volumetric Modulated Arc Therapy (VMAT) was introduced [41]. This treatment involves a dynamically modulated arc of up to 360 degrees, where the entire dose volume is delivered in a single source rotation. During the optimisation process, the motion of the MLC and the number of Monitor Units (MU) per degree of gantry rotation are restricted to ensure that the gantry rotation speed, leaf translation speed, and dose rate maxima do not excessively limit the delivery efficiency. Plans generated with VMAT optimisation exhibit dose distributions equivalent to or superior to static gantry IMRT [42]. Today, the delivery time for a 2 Gy per fraction is reduced to 1-2 minutes.

The radiotherapy treatment planning process

Medical dosimetrist

Ion chambers were invented and developed during the 1940s, leading to the emergence of direct dose measurement in water and the birth of dosimetry in radiotherapy. In the 1950s and 1960s, treatment planning became more accurate by utilising detailed physical accuracy and dosimetry. Close collaboration between the radiation oncologist and medical physicists was vital for planning individual therapy courses. As more patients received radiotherapy, the time spent on dose planning became a large proportion of the treatment preparation. A new team member, the 'medical dosimetrist,' was introduced. Institutions with sufficient numbers of medical physicists and medical dosimetrists working in coordination with radiation oncologists and using MV equipment became standard practice [43].

Medical professionals used to plan radiation therapy manually before computer-aided planning technology was introduced. The first dose plans were created by hand on transparent paper. The contour of the body cross-section was outlined

manually, and the internal structures like the lungs and skeleton were identified manually as well. Predefined isodose lines were drawn on the paper to determine energy with or without wedges. Any corrections for body contour or OARs were made using simple scaling factors. Next, the desired isodose curves were added from various angles, and the cumulative dose was drawn manually. In the 1960s, attempts were made to automate this process using computers [44, 45]. Initially, the process was similar to manual planning, where the isodose curves were divided into a grid pattern, each grid with a percentage dose value. The body cross-section was also divided into grids, and the computer calculated the dose in each box based on the selected gantry angles. Finally, the isodose curves for the finished dose plan could be plotted based on this information [46]. During the 1960s and early 1970s, the increasing sophistication of computerised treatment planning continued [47].

Imaging for radiotherapy treatment planning

In 1972, Allan McLeod Cormack and Godfrey Hounsfield proposed the theoretical and experimental work that led to the development of the first commercial Computed Tomography (CT) scanner [48].

This development was pivotal in the treatment planning field. CT provides several advantages over planar, two-dimensional (2D) X-ray imaging: a) provides precise cross-sectional depictions of the body; b) it effectively illustrates the internal anatomical structures; c) ability to detect the existence and the degree of tumour involvement is present in internal organs; d) it allows for the quantitative measurement of X-ray absorption in anatomical structures by converting Hounsfield Units (HU) to electron density (ED), which in turn enables dose calculations with inhomogeneity corrections by the treatment planning system (TPS); e) it allows for non-invasive monitoring of a tumour's response to treatment [49-51].

In the 1970s, there was a shift in radiation therapy planning from 2D to 3D, the latter commonly referred to as three-dimensional conformal radiotherapy (3D-CRT) [52-54]. This advancement increased precision in targeting tumours and minimising damage to nearby organs. As computing power and software improved, 3D-CRT planning became more common, including cerrobend blocks, dynamic wedges, and the development of the Beam's Eye View (BEV) concept. By the mid-1980s, 3D-CRT planning had become routine in clinical use [55].

In modern radiotherapy workflows, relying on a combination of CT and Magnetic Resonance Imaging (MRI) is typical. CT scans provide crucial ED data utilised in treatment planning, while MRI scans, renowned for their exceptional soft tissue contrast, serve as valuable aids in delineating targets and OAR [56].

3D-CRT treatment planning

The planning process for 3D-CRT is based on manual work wherein the medical dosimetrist attempts to manually optimise the dose distribution, typically relying on some predefined dose/volume objectives/constraints. The medical dosimetrist navigates through a trial-and-error process, adding new parameters or changing existing ones, calculating the dose, and making changes until the dose distribution is as good as possible without making the delivery of the plan too complicated. The parameters that the medical dosimetrist can work within the 3D-CRT planning process are the number of treatment beams, energy, gantry angle, collimator angle, the beam shape from the MLC, and the weight of each beam. Additional fields that cover only parts of the target and have lower weight to even out the dose can also be added. Additionally, the medical dosimetrist can add a wedge on one or more fields and change the weight of the wedged beam.

3D-CRT is becoming less common in modern radiotherapy. VMAT technology has evolved regarding conformal dose distribution, sparing OARs, and delivery speed. In our clinic, only breast cancer treatments and palliative treatments are primarily still given with 3D-CRT technology.

VMAT treatment planning

In contrast to the forward treatment planning for 3D-CRT described earlier, VMAT treatment planning is an inverse treatment planning process. Inverse treatment planning employs a computational approach to achieve specific treatment objectives while adhering to constraints to minimise dose to healthy tissues. The primary aim is to deliver a therapeutic dose to the tumour while sparing adjacent normal tissues. Constraints, such as minimum dose to the target, maximum doses to critical organs, or tolerance limits for healthy tissues, are incorporated into the optimisation. This algorithm iteratively adjusts beam angles, intensities, and other parameters to find the optimal dose distribution that balances treatment efficacy with minimising side effects.[57-60].

The medical dosimetrist can change the objectives during optimisation to improve plan quality. Examples of other helpful optimiser tools in the treatment planning system include the Normal Tissue Objective (NTO), which reduces dose outside of the target, and the Monitor units (MU) objective, which can minimise the number of MUs and thereby reduce the complexity of the plan, and the Base Dose Plan function, which allows the optimiser to consider the dose previously given to the patient [3]. The Base Dose Plan function was essential for the adaptive VMAT planning in the PROPER 1 study. This function is thoroughly discussed and explained in the chapter: 'Radiotherapy treatment planning in the PROPER 1 trial' and the appendix.

Fractionation in external beam radiotherapy - the linear quadratic model

How the total dose is fractionated over external beam RT significantly influences tumour response and side effects. The linear quadratic model, often referred to as the LQ model, is commonly used to describe and evaluate cell survival and the response of biological tissues to radiation [61]. As the name of the mathematical model suggests, it contains a linear (α) and a quadratic component (β). The surviving fraction, S, of cells after a single dose D of radiation can then be described as

$$S = e^{-(\alpha D + \beta D^2)}$$

or

$$-\ln(S) = \alpha D + \beta D^2$$

Where α and β are constants, the linear component often represents irreparable cell damage, while the quadratic component means reparable damage. These assumptions may not necessarily be accurate, and the LQ model can be seen as fitting cell survival with a second-degree polynomial. Nevertheless, the ratio of the constants, i.e., the α/β ratio (unit Gy), is most useful as it reflects the "bendiness" of the cell survival curve (Figure 1).

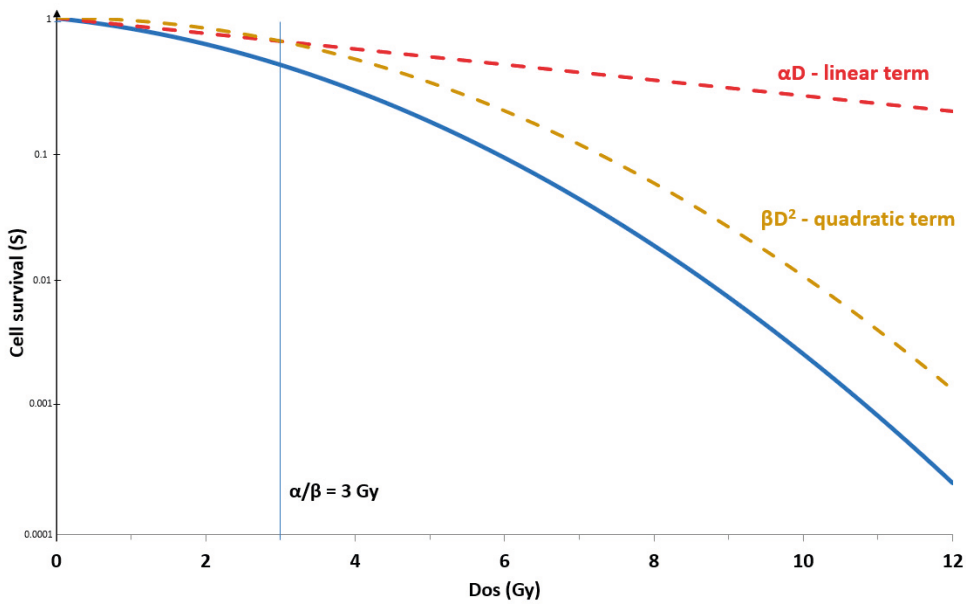

Figure 1. Cell survival (S) as a function of exposure to single doses (D). At low doses, the survival is dominated by the linear term, while at higher doses, the quadratic term becomes more important. When these effects are equal, the dose equals α/β (3 Gy). *©Vilberg Jóhannesson*

If the total dose D is instead given in n fraction of dose d each, assuming complete repair between the fractions and neglecting any cell proliferation, the cell survival becomes

$$-\ln(S) = n(\alpha d + \beta d^2) = D(\alpha + \beta d)$$

The LQ concept can be applied in a clinical setting for tumour and normal tissue response by assuming that the biological effect is proportional to -ln (and then also to -ln(S) / α as α is a constant), leading to the concept of Biologically Effective Dose [62], derived from the basic LQ-equation as

$$BED = D(1 + \frac{d}{\alpha/\beta})$$

The knowledge of tissue-specific α/β ratios is therefore crucial in radiation oncology and radiobiology when studying the effects of changes in fractionation schedules. Figure 2 illustrates the impact of fractionation for tissues with two different α/β ratios.

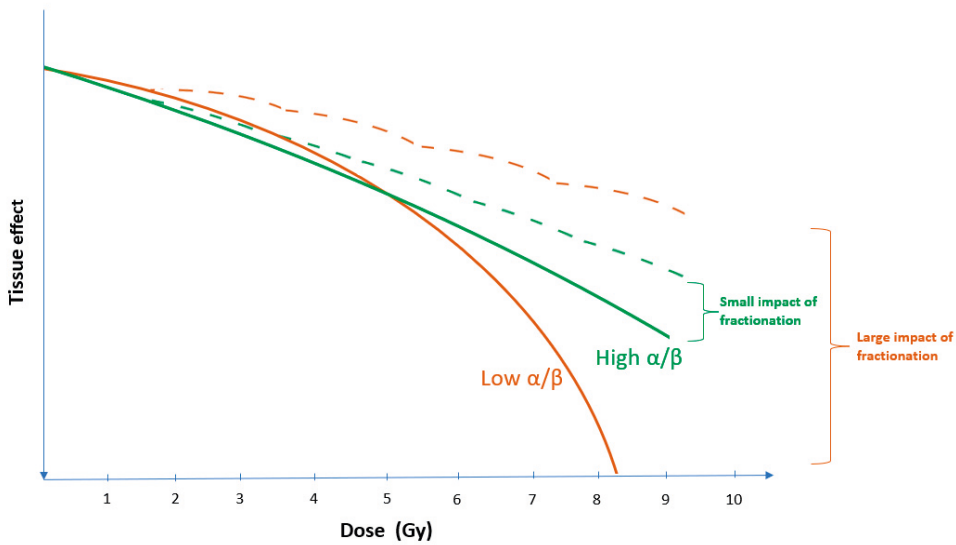

Figure 2. The effect of fractionation for tissues with two different α/β ratios: "high" α/β = 10 Gy and "low" α/β = 3 Gy. High α/β (green solid line) have nearly constant rates of cell killing with increasing single fraction dose, while low α/β (brown solid line) shows a pronounced curvature, with greater killing per unit dose at higher single fraction dose. When the dose is delivered in five fractions (dashed lines), it has a smaller impact when the α/β ratio is high compared with a low α/β ratio. *©Vilberg Jóhannesson*

For example, the BED concept can be used, e.g. to compare the effects of different fractionation schemes. A commonly used approach is to convert an arbitrary fractionation schedule (delivered in n fractions of dose d to a total dose D) to a conventional fractionation schedule delivered with 2 Gy fractions. The "Equivalent Total Dose at 2 Gy" (EQD2) is then obtained by equating their BEDs, resulting in

$$EQD2 = D \times \left(\frac{d + \alpha/\beta}{2 + \alpha/\beta} \right)$$

It should be noted that the basic BED equation does not account for a tumour or tissue proliferation and, consequently, may not accurately reflect the effects of fractionation schedules, with significant differences in total treatment time, for rapidly proliferating tissues. The concept can address this limitation by incorporating a time correction factor [62].

The EQD2 concept has been used in all four studies in this thesis.

Prostate cancer

Epidemiology

The number of men diagnosed with prostate cancer in Sweden has tripled over the past 20 years, with approximately 125,000 men living with the diagnosis in 2021 and about 10,000 new cases reported every year. This increase is attributed to a combination of factors, including the ageing population, earlier detection of prostate cancer, and improved treatment options that enable men with advanced prostate cancer to live longer [63]. One in five Swedish men is diagnosed with prostate cancer in their lifetime, and it is rare for the disease to occur before the age of 50. Diagnostic activity has reduced the median age at diagnosis from 74 to 69 years between 1995 and 2005. The National Prostate Cancer Registry provides detailed information on incidence, disease characteristics, and primary treatment [64].

Diagnostic methods

PSA Test (Prostate-Specific Antigen)

PSA is a protein produced by the prostate gland that can be measured in a blood test. If the PSA levels are high, it may indicate the presence of prostate cancer. However, other conditions like benign prostatic hyperplasia or prostatitis can also cause elevated PSA levels. PSA levels vary between different age groups, with higher reference levels for older men. After prostatectomy, PSA levels should decrease to unmeasurable levels, commonly defined as < 0.1ng/ml. A measurable and rising PSA after surgery is a strong indicator of a tumour recurrence. [63].

Transrectal Ultrasound (TRUS):

A small probe is inserted into the rectum to obtain ultrasound images of the prostate. TRUS may be used to guide prostate biopsies [63, 65].

MRI (Magnetic Resonance Imaging)

MRI scans may provide detailed images of the prostate gland and surrounding tissues. MRI can help detect suspicious areas within the prostate that may require further investigation, such as targeted biopsies. Additionally, MRI is used for staging purposes to determine the extent of the spread of cancer, which is essential for choosing the appropriate treatment [66].

^{68}Ga-PSMA-PET/CT

Positron emission tomography (PET) tracers, like ^{68}Gallium-Prostate-Specific-Membrane-Antigen-HBED-CC-ligand (^{68}Ga-PSMA-11), have shown great promise

in detecting prostate cancer lesions [67, 68]. These tracers bind to and inhibit the prostate-specific membrane antigen (PSMA), resulting in a higher detection rate of tumour manifestations than previous tracers. This could improve patient selection for curatively intended treatment with SRT, which can now be extended to include regional lymph nodes and boost local recurrence [9, 67-70].

Biopsy:

If PSA levels are elevated or if there are abnormalities found during a rectal exam, a biopsy may be performed. During a biopsy, small samples of prostate tissue are taken using a needle, usually guided by ultrasound imaging. A pathologist examines these tissue samples under a microscope to determine if cancer cells are present. The Gleason score, based on the appearance of the cancer cells in the biopsy samples, is used to grade the aggressiveness of the cancer [63].

Prostate cancer staging

Gleason Score

Gleason score is a grading system used to evaluate the aggressiveness of prostate cancer based on the appearance of cancer cells in a biopsy sample. The score ranges from 6 to 10, with lower scores indicating less aggressive cancer and higher scores indicating more aggressive cancer. It is determined by examining the two most prevalent patterns of cancer cells in the biopsy sample, assigning a grade to each pattern, and summing the two grades to obtain the Gleason score [71].

TNM Staging System

Once prostate cancer is confirmed, it is staged using the TNM staging system. This system categorises the tumour based on its size and extent (T), whether it has spread to nearby lymph nodes (N), and whether it has metastasised to distant organs (M). The TNM staging system helps guide treatment decisions and prognosis [72].

Risk groups

Prostate cancer without known spread is divided into risk groups based on PSA value, TNM classification and Gleason sum (Table 1).

Table 1. The risk group classification according to the Swedish National Care Program for prostate cancer [63].

Very low risk	T1**c**
	Gleason score 6, ≤ 8 mm cancer in total 1–4 av 8–12 systematic biopsy cores
	PSA <10 ng/mL och PSA-density <0,15 ng/mL/cm3
Other low risk	T1 or T2a
	Gleason score 6 and
	PSA <10 ng/mL which does not meet the criteria for very low risk
Favorable intermediate risk	One of the following risk factors:
	T2b or T2c
	Gleason score 3+4
	PSA 10–19 ng/mL
Unfavorable intermediate risk	>1 of the above risk factors or
	Gleason score 4+3 or
	Gleason score 3+4 in more than 50% of the systematic biopsy cores.
High risk	T3a or strong suspicion of extraprostatic growth on MRI (EPE) [73] or
	Gleason score 8 or
	PSA 20 - 39 ng/mL
Very high risk	2-3 of the above risk factors or
	T3b or T4 or
	Gleason score 9-10 or
	PSA ≥40 ng/mL

Primary treatments for prostate cancer

Radiotherapy (RT) can be carried out as external beam RT, brachytherapy (BT) or a combination of both [74].

External beam RT can be used to treat patients with low-, intermediate- or high-risk disease. Advanced radiotherapy techniques such as IMRT or VMAT are commonly used for treating prostate cancer due to their ability to deliver conformal radiation dose distributions. The position of the prostate gland can vary based on the fullness of the bladder and rectum. Image-guided techniques based on implanted gold fiducials are used to ensure adequate dose coverage with tight treatment margins.

BT is a type of RT where the radioactive source is placed inside or next to the volume that needs treatment, the prostate in this case. The two methods of BT delivery are high dose rate brachytherapy (HDR-BT) or low dose rate brachytherapy (LDR-BT), and both require the patient to be under anaesthesia to insert the sources. The guidance for implantation is done using TRUS. During the process, the urethra and the rectum are the primary OARs. BT can be used alone or in combination with external beam RT.

Surgery (Radical Prostatectomy (RP)): Robot-assisted laparoscopic surgery has become the standard of care for prostate cancer. This treatment involves the surgical removal of the prostate gland and may also include lymph node extraction for patients at increased risk of lymph node spread, primarily those with high-risk disease. Depending on the extent of the tumour, surrounding tissues may also need to be removed. A pathological examination will determine whether the procedure was considered radical. In cases of positive surgical margins, the risk of recurrence is increased [75].

Hormone Therapy (Androgen Deprivation Therapy – (ADT)): Hormone-sensitive prostate cancer patients often receive ADT treatment in the palliative setting. In the curative setting, neoadjuvant and adjuvant ADT is combined with RT for high-risk patients because it has been found to have a synergistic effect by preventing DNA repair [76].

Hypofractionation in prostate cancer treatment

The α/β ratio of prostate cancer is low (1.5-3.0 Gy) compared to many other tumours [27], i.e., even possibly lower than the α/β ratio for late normal tissue reactions [77-79]. This implies that hypofractionation should be more effective (and cost-efficient) than conventional fractionation [80]. Consequently, this concept has driven the development of two main approaches: moderate hypofractionation, typically delivering 2.4-3.4 Gy per fraction, and ultra-hypofractionation (UHF), using 5 Gy or more per fraction [81]. UHF is also referred to as extreme hypofractionation, stereotactic body radiation therapy (SBRT), or stereotactic ablative radiotherapy.

It is unclear whether the α/β ratio is independent of fraction size and whether the LQ model suits very high doses per fraction. It has been suggested that the α/β ratio increases with dose per fraction [27, 82].

The HYPO-RT-PC trial [32] was the first trial to compare the effectiveness and tolerability of image-guided UHF and CF external beam radiotherapy without any androgen deprivation therapy for patients with intermediate to high-risk prostate cancer. The study shows that UHF radiotherapy is equally effective for intermediate-to-high-risk prostate cancer regarding failure-free survival. Although early side effects are more apparent with UHF, late toxicity remains the same as CF. These results favour the use of UHF in prostate cancer radiotherapy.

According to the Swedish National Care Program for prostate cancer, UHF radiotherapy is recommended as primary treatment for intermediate and high-risk prostate cancer patients unless it is deemed necessary to include seminal vesicles [63].

Biochemical recurrence after radical prostatectomy

Elevated levels of PSA that are observed during post-radical prostatectomy monitoring, can indicate an early relapse of prostate cancer (biochemical recurrence (BCR)). In cases of BCR where there is no radiological evidence of tumours beyond the prostate, it is often assumed to be a local recurrence. Around 20-40% of prostate cancer patients experience BCR [83] of the disease after undergoing surgical treatment. This is usually confirmed through a second PSA measurement above 0.2 ng/mL [84], and the preferred treatment option for BCR is SRT [85-87]. Typically, SRT involves irradiation of the prostate bed with 64-70 Gy in 33-35 fractions [87-90]. Recent evidence suggests that pelvic lymph node radiotherapy (PLNRT) and hormonal therapy can improve the outcome of SRT [8, 91].

Approximately half of SRT patients achieve complete biochemical remission 3-5 years after the treatment [92]. However, SRT can fail due to a target miss, radiation-resistant cancer, insufficient dosage or because of nodal or distant metastases. Predictive factors, including pre-treatment clinical factors, can determine the outcome of SRT [83, 93-95]. These factors are included in a nomogram developed by Stephenson et al. [7], which calculates the probability of remaining free from disease progression six years after SRT. This information can be used to select patients for SRT.

The PSA study

Monitoring PSA change during SRT could be an effective method to improve the identification of high-risk patients who are more likely to benefit from treatment escalation like PLNRT. This enrichment strategy is widely used in medical oncology trials to avoid diluting treatment effects [96, 97]. For example, patients who do not experience a PSA response during early SRT could be considered for the addition of PLNRT. However, whether PSA change during radiotherapy improves the predictive performance of previously recognised clinical pre-treatment parameters, as included in the nomogram described by Stephenson et al. [7], is not previously well studied.

The PSA study [98] aimed to evaluate the predictive value of PSA response during SRT and its impact on treatment outcomes in relation to previously established prediction parameters. The trial demonstrated that PSA decay during SRT is an independent, strong predictor of long-term biochemical control. The long-term goal is to implement this information in an enrichment trial set-up and subsequently in clinical use.

Methods

The PROPER 1 trial (Papers I-III)

Study design

The PROPER 1 (PROspective evaluation of 68-Ga-PSMA-PET and early PSA kinetics during salvage radiotherapy for PERsonalising the management of men with relapse of prostate cancer after radical prostatectomy) trial is a phase II study conducted at Skåne University Hospital in Sweden. It is an open-label, prospective trial with the objective, based on early PSA response during salvage radiotherapy, to personalise the treatment and evaluate a new novel imaging method, PSMA-PET.

The trial's primary objective was to evaluate a new adaptive treatment strategy involving sequential PLNRT and boost to PSMA-PET-positive lesions guided by PSA kinetics during SRT as a biomarker.

Eligible for inclusion were patients at least 18 years old with confirmed prostate cancer in the prostatectomy specimen, with any pT, pN0/Nx, M0, and a confirmatory PSA level of ≥ 0.15 ng/mL. Additionally, they should have a WHO performance status of 0-1 and adequate laboratory findings according to protocol.

A PSA drop below 0.15 ng/mL after five weeks of SRT was found to be the strongest predictor of short-term outcome (PSA < 0.1 ng/mL one-year post-SRT) from the PSA study at the time of trial design [98] and was therefore used to differentiate responders from non-responders.

^{68}Ga-PSMA-PET/CT

Before the start of SRT, a ^{68}Ga-PSMA-PET/CT scan was performed (2.5 MBq per kilogram of body weight, up to a maximum of 300 MBq). The scan results were assessed before the time of treatment adaptation. Any uptake patterns deviating from normal physiological activity were registered as indicative of potential malignancy.

Adaptive salvage radiotherapy

At first, 70 Gy in 35 fractions was prescribed to the prostate bed only. Baseline PSA was measured on the first day of RT and then weekly after that. Patients were defined as responders if the PSA level had dropped below 0.15 ng/mL after 50 Gy, i.e. five weeks of treatment. Patients were defined as non-responders if the PSA level was still ≥ 0.15 ng/ml.

The initial prescription of 70 Gy to the prostate bed was administered to responders, regardless of PSMA-PET findings. In case of non-response, a new prescription was defined that included the initial 70 Gy to the prostate bed, along with an additional 50 Gy in 25 fractions to adjuvant lymph nodes. Non-responders who had lymph node metastases on pre-therapy PSMA-PET received a boost of 60 Gy in 25 fractions, while local recurrence was treated with a dose corresponding to EQD2 α/β=3 Gy of 74–78 Gy. Patients with distant metastases or more than three lymph node metastases on PSMA-PET were excluded from further SRT and referred to standard of care treatment for metastatic disease (Figure 3).

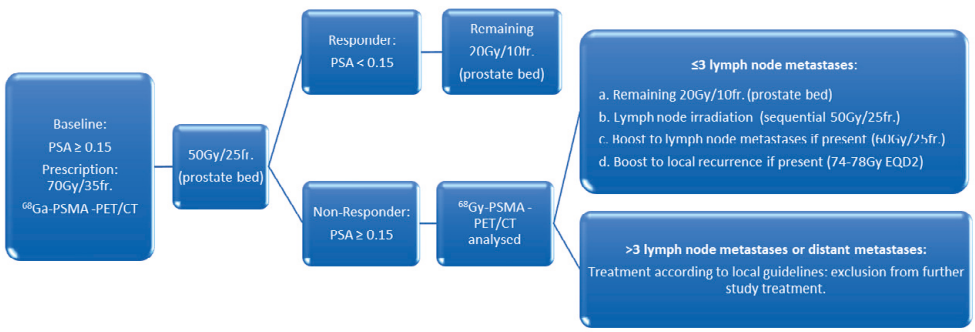

Figure 3. Overview of the treatment schedule in the PROPER 1 trial, from baseline to the division into responder and non-responder.*Figure from Paper II.*

PSA levels were monitored after SRT. A confirmed increase in PSA level of 0.2 ng/mL above post-SRT nadir or a clinical recurrence was considered as treatment failure. Urinary and bowel toxicity was evaluated according to the RTOG toxicity scale [99] by physicians at baseline, at the end of SRT, at 3 and 12 months after the end of SRT. Quality of life was evaluated using the EORTC QLQ-C30 [100] and QLQ-PR25 [101] questionnaires at baseline, at the end of SRT and 12 months after SRT.

Radiotherapy treatment planning in the PROPER 1 trial

The Radiotherapy treatment planning in the PROPER 1 trial was carried out in Eclipse versions 13.6 and 15.6 (Varian Medical Systems, Palo Alto, CA, USA) [3] with the anisotropic analytical algorithm versions 10.0.28 and 13.6.23, and the photon optimisation algorithm versions 10.0.28 and 13.6.23 (Paper I).

Plan 1 was created for the prostate bed, PTV-P, to deliver 70.0 Gy in 35 fractions. The isocenter is positioned at the centre of the most cranial slice of PTV-P to minimise dose divergence in plan 3 if non-responder. The plan was normalised to the median PTV dose, ensuring a smooth, homogeneous dose distribution with a maximum dose of less than 103% in the cranial part of PTV-P, crucial to limiting the maximum dose at the inter-phase junction in the event of non-response.

After five weeks of treatment, responders continued with plan 1. In the case of non-responders, a copy of plan one was made, and the fractionation was changed to 50.0 Gy in 25 fractions. This copy was then used as a base plan in the optimisation of plan 3.

Plan 2 was created for the prostate bed, PTV-P and adjuvant lymph nodes, PTV-N, to receive 20,0 Gy in 10 fractions. If present, lymph node metastases, PTV-Lmet, received 24.0 Gy, and an individualised boost was administered in cases of local recurrence, PTV-T. To achieve high dose conformity to the target and spare the OARs, a maximum field size of about 15 cm in the MLC direction was used due to the equipment's limitations. This was achieved by decreasing X1 for arc one to obtain a field size of 15 cm and vice versa for X2 in arc two, where X1 and X2 are defined in the IEC 61217 coordinate system [102] (Figure 4). The plan was normalised to the median PTV dose.

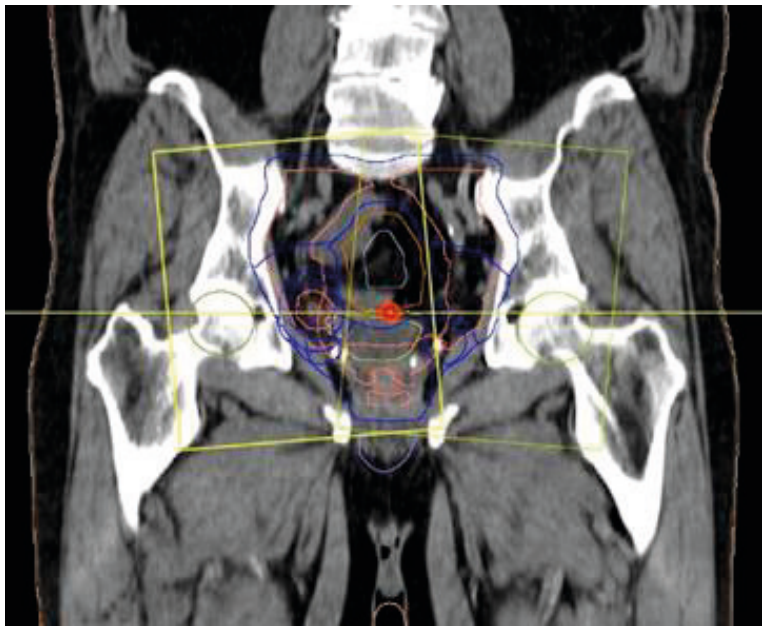

Figure 4. A field size of about 15 cm in the MLC direction (yellow square) was used due to the limitations of the MLC movements. *©Vilberg Jóhannesson*

Plan 3 was created for the lymph nodes, PTV-N, to receive 30.0 Gy in 15 fractions and 36.0 Gy to lymph node metastases, PTV-Lmet if present. In optimising plan 3, the Base Dose Plan function in Eclipse accounted for the dose from a previous plan. A copy of plan one was used as the base plan. The field width was decreased to about 15 cm, as in plan 2. No plan normalisation was applied. This process was further developed during the study by including an $EQD2_{\alpha/\beta=3}$ correction of the dose distribution from plan 1. The physical dose distribution in plan one was converted to EQD2 with $\alpha/\beta=3.0$ Gy for both tumour and normal tissues. This was performed with an in-house software that multiplied the total physical dose in each voxel of the dose matrix by the EQD2 correction factor.

The adaptive sequential plan-on-plan VMAT radiotherapy treatment planning technique used for all patients in the PROPER 1 trial, as defined by the author and the study team, is described in detail in the appendix.

Organs at risk delineation

Weekly CBCT images were used to outline OARs in Paper III. The inferior border of the rectum was delineated from the lowest level of the ischial tuberosities to the point where it loses its round shape in the axial plane and connects anteriorly with the sigmoid [103]. The bladder was outlined from its base to the dome, and the most

caudal slice of the bladder remained the same in all CBCTs, as it was hard to define the caudal limit of the bladder on the CBCTs. The bladder trigone was described as a sub-volume of the bladder wall, which ranged between the right and left ureteral orifices and the urethral orifice and was created by adding an inner margin of 5 mm to the contoured bladder (Figure 5). The anal canal was outlined as the distal 4 cm of the rectum, which was a sub-volume of the rectum.

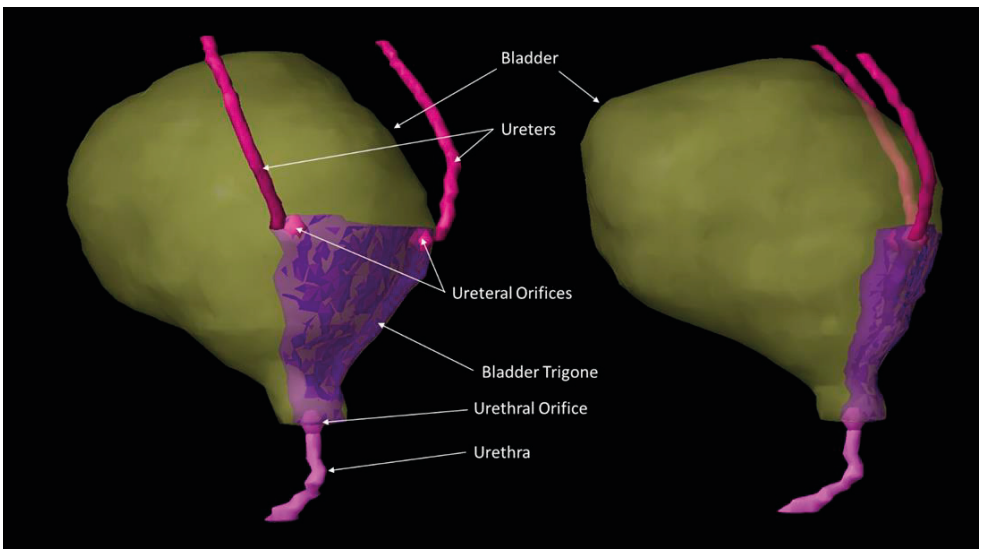

Figure 5. Images of the urinary bladder and bladder trigone from a posterior and lateral view. *©Vilberg Jóhannesson*

Planned versus estimated delivered radiation doses

Rigid registration from the treatment system was used as a base for performing the DIR between the planning CT and CBCT, with the planning CT as the reference. The rectum and bladder were outlined separately in the planning CT and CBCT images to fine-tune the DIR settings. The DIR quality was assessed using the volumetric Dice similarity coefficient (vDSC) for the rectum and the bladder, and cases with low vDSC values were visually examined. The vDSC was quantitatively evaluated based on the American Association of Physicists in Medicine recommendations in task group 132 (AAPM TG132) [104]. The DIR for each weekly CBCT registration was applied to the planned dose distribution to obtain an estimated dose distribution in the CT geometry. These estimates were summed to represent the spatial delivered dose distribution received over the whole treatment course (Paper III).

In the analysis of dose distribution and side effects, various dose-volume metrics were examined for both the rectum/anal canal and bladder/trigone. The metrics used for the rectum/anal canal included V_{50Gy}, V_{60Gy}, V_{65Gy}, V_{70Gy}, and $D_{2\%}$. Meanwhile, the metrics used for the bladder and bladder trigone included V_{65Gy}, V_{70Gy}, $D_{2\%}$, and D_{mean}.

We compared dose-volume metrics for planned versus estimated delivered doses to OARs. We also investigated the association between these metrics and urinary and bowel RTOG grade ≥ 2 toxicity, as well as Patient Reported Outcome Measures ($PROM_{10\%}$) [105, 106]. We compared the dose-volume metrics for patients who experienced RTOG grade ≥ 2 toxicity and those who did not, as well as patients who reported changes in urinary/bowel symptoms $PROM_{10\%}$ and those who did not report such changes.

Ultra-hypofractionated radiotherapy for prostate cancer, including seminal vesicles (Paper IV)

Patients and segmentation

The treatment planning study in Paper IV is based on thirty consecutive prostate cancer patients treated at Skåne University Hospital, Lund, Sweden, who received UHF radiotherapy within the HYPO-RT-PC study [32].

The CTV for the prostate was defined as CTV_{pros} on CT with MR guidance. PTV_{pros} was created by adding an isotropic margin of 7 mm to the CTV_{pros}. The present guidelines for determining the CTV vary for the seminal vesicles, but typically, the recommendation is to include the proximal 10-20 mm of the SV or the entire SV in case of seminal vesicle invasion (SVI) [107]. Therefore, two CTVs for the proximal parts of the SV were retrospectively defined (CTV_{ves} 10mm and CTV_{ves} 20mm). PTV_{ves} 10 and 20 mm were contoured by adding an isotropic margin of 10 mm to the CTV_{ves}. The rectum and bladder were redefined following the pelvic normal tissue contouring guidelines of RTOG [103]. In addition, the bladder trigone was defined as a triangular sub-volume of 5 mm thick bladder wall between the right and left urethral orifice and the urethral orifice [19] (Figure 6).

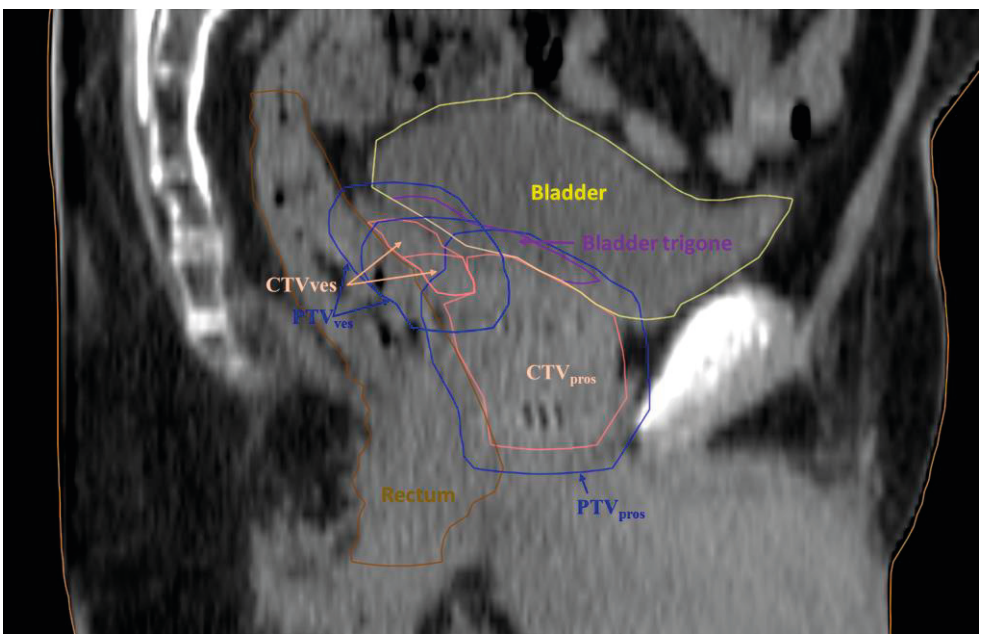

Figure 6. Targets; CTV_{pros} + PTV_{pros}, CTV_{ves} 10 and 20 mm + PTV_{ves}. OARs; rectum, bladder and bladder trigone as defined in Paper IV. *©Vilberg Jóhannesson*

Prescribed doses

The clinical practice at Skåne University Hospital includes SV in our CF schedule if the statistical risk of SVI is over 20%. The RT is administered as a sequential boost with 78.0 Gy in 39 fractions to the prostate, 50.0 Gy in 25 fractions to the elective SV, and 70.0 Gy in 35 fractions for confirmed SVI.

The HYPO-RT-PC study suggests an α/β ratio close to 3 Gy for tumour response and late toxicity in normal tissue[32]. According to the meta-analysis conducted by Vogelius and Bentzen, the best estimate of the α/β ratio is 1.6 Gy (95% CI 1.3-2.0 Gy)[27]. As discussed above, it might be slightly higher for UHF. In paper IV, we employed α/β ratios of 2.0 Gy and 3.0 Gy to design equi-effective treatment schedules for the SV using the linear-quadric model, where D represents the total prescribed dose, and d is the dose per fraction.

$$EQD2 = D \times \left(\frac{d + \alpha/\beta}{2 + \alpha/\beta} \right)$$

The prescribed ultra-hypofractionated simultaneous integrated boost (UHF-SIB) fractionation in paper IV was 7 fr. with 3 fr. per week for 2.5 weeks with the following doses:

Prostate: 42.7 Gy, equivalent to 78.0 Gy in 35 fr. for α/β=3 Gy, and
confirmed SVI: 37.8 Gy, equivalent to 70 Gy in 35 fr. for α/β=2 Gy, or
confirmed SVI: 40.1 Gy, equivalent to 70 Gy in 35 fr. for α/β=3 Gy, or
elective SV: 31.2 Gy, equivalent to 50 Gy in 25 fr. for α/β=2 Gy, or
Elective SV: 32.7 Gy, equivalent to 50 Gy in 25 fr. for α/β=3 Gy.

Radiation treatment planning

The planning of CT-based VMAT was performed using Eclipse version 15.6 (Varian Medical Systems, Palo Alto, CA, USA) with version 15.6.05 of the anisotropic analytical algorithm and photon optimisation algorithm (PO). The optimisation and calculation grid sizes were 2.5 mm, and the aperture shape controller "very low" was used in the PO. Two full 10 MV arcs with collimator rotation of five degrees and a complementary collimator angle for the second arc were used. Constant parameters, lower and upper, were used for all target structures in every plan. "Target Autocrop" [108] managed overlapping target structures in the SIB plans. The following three OAR help structures were utilised: bladder, excluding the target with a 5 mm margin; rectum, with an isotropic 5 mm margin, excluding the target with a 5 mm margin; and rectum volume that overlaps the target. The "Normal Tissue Objective" (NTO) function in Eclipse was employed for all plans with identical manual settings of all parameters. The plan optimisations began with only target and NTO objectives active and were optimised through "MR

level 1" before pausing the optimisation. At this stage, the optimisation objectives for each OAR were included, and the priority value was adjusted to suit the current plan. Every OAR was optimised to minimise the dose as much as possible without compromising the target coverage. All plans were optimised at least twice throughout all four "MR levels". After the final dose calculation, the plan was normalised to the prescribed median dose of PTV_{pros}.

The following 15 treatment plans were created for each patient:

1. PTV_{pros} 42.7 Gy / 7 fr
2. PTV_{pros} 42.7 Gy and PTV_{ves} 10 mm 37.8 Gy / 7 fr.
3. PTV_{pros} 42.7 Gy and PTV_{ves} 20 mm 37.8 Gy / 7 fr.
4. PTV_{pros} 42.7 Gy and PTV_{ves} 10 mm 40.1 Gy / 7 fr.
5. PTV_{pros} 42.7 Gy and PTV_{ves} 20 mm 40.1 Gy / 7 fr.
6. PTV_{pros} 42.7 Gy and PTV_{ves} 10 mm 31.2 Gy / 7 fr.
7. PTV_{pros} 42.7 Gy and PTV_{ves} 20 mm 31.2 Gy / 7 fr.
8. PTV_{pros} 42.7 Gy and PTV_{ves} 10 mm 32.7 Gy / 7 fr.
9. PTV_{pros} 42.7 Gy and PTV_{ves} 20 mm 32.7 Gy / 7 fr.
10. PTV_{pros} and PTV_{ves} 10 mm 70.0 Gy / 35 fr.
11. PTV_{pros} and PTV_{ves} 20 mm 70.0 Gy / 35 fr.
12. PTV_{pros} 8.0 Gy / 4 fr.
    a. Plan sum: 10+12
    b. Plan sum: 11+12
13. PTV_{pros} and PTV_{ves} 10 mm 50.0 Gy / 25 fr.
14. PTV_{pros} and PTV_{ves} 20 mm 50.0 Gy / 25 fr.
15. PTV_{pros} 28.0 Gy / 14 fr.
    a. Plan sum: 13+15
    b. Plan sum: 14+15

Results

The PROPER 1 trial (Papers I-III)

Clinical outcome

The study inclusion was between March 2016 and December 2019. After excluding two patients who withdrew consent and one with more than three lymph node metastases, 97 patients were analysed with a median follow-up of 38 months. Of these, 35% were responders (PSA < 0.15 ng/mL after 50 Gy), and 65% were non-responders (PSA ≥ 0.15 ng/mL after 50 Gy). The cohort's three-year failure-free survival (FFS) was 76%, 94% for responders and 68% for non-responders. While treatment-related toxicity was similar between the groups, non-responders showed a tendency towards increased acute bowel toxicity, and their patient-reported diarrhea scores were significantly higher.

PSMA-PET findings revealed an overall detection rate of 26%, with a significant difference between responders, three patients (9%) and non-responders, 22 patients (35%). Nine patients had a local recurrence.

Ten patients had findings in the pelvic lymph nodes, one of which was a responder that later was shown to be a false positive finding. The nine patients in the non-responder group received a boost to the lymph node metastases.

Six patients, one in the responder group and five in the non-responder group had findings in bone and/or liver. During the five weeks of SRT before response evaluation, we evaluated these findings with further imaging and histological assessment. In all cases, we could confirm that they were false positive findings.

Radiotherapy treatment planning

The first 35 out of 64 patients treated without adjusting for fractionation effects of the base plan all had target coverage where the criteria were met in physical dose. However, when the equivalent dose in 2 Gy fractions ($EQD2_{\alpha/\beta=3}$) was applied, all dose-volume criteria were met except for the CTV-N and PTV-N. The dose coverage for these nodal volumes in the inter-phase junction was slightly below the recommended dose-volume criteria. A statistically significant improvement in dose

coverage ($P < 0.0001$) was observed in the remaining 29 patients when an $EQD2_{\alpha/\beta=3}$-corrected base plan was introduced, compared to those treated without an $EQD2_{\alpha/\beta=3}$ correction of the base plan. This improvement in target coverage was achieved without increasing doses to the organs at risk (Figure 7).

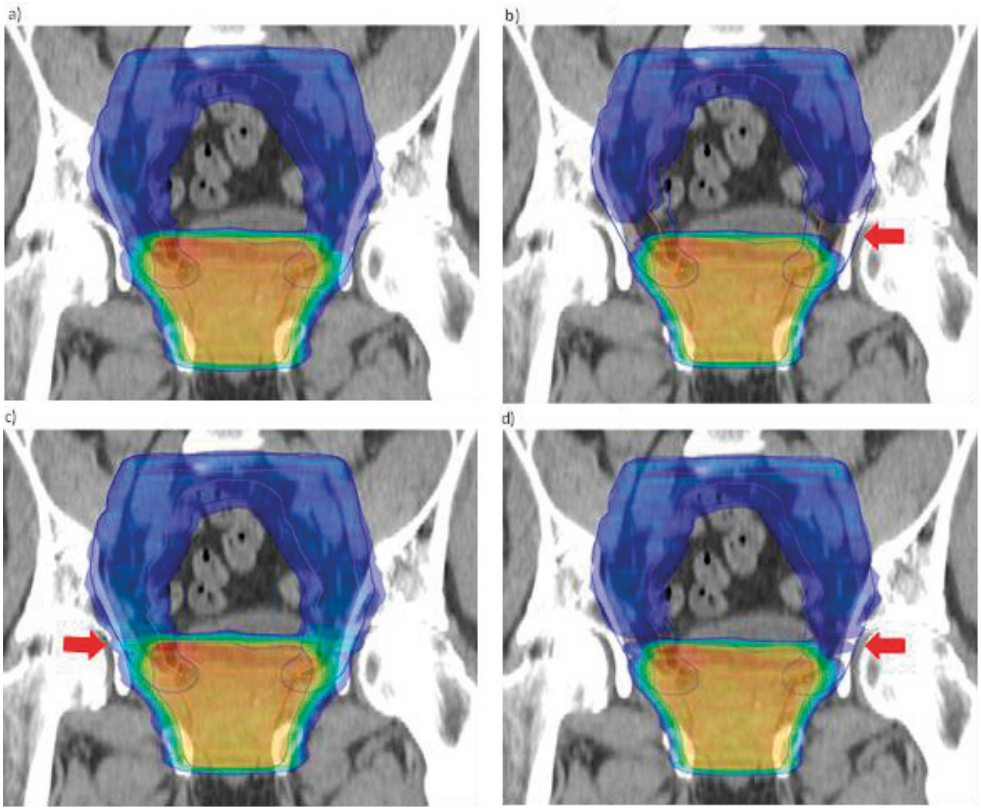

Figure 7. Summed dose distributions for plans 1–3. (a) Dose distribution in physical dose and the base plan in physical dose. All target objectives are fulfilled. (b) Dose distribution EQD2-corrected, showing lower target coverage in the inter-phase junction (red arrow). (c) Dose distribution in physical dose and the base plan EQD2-corrected. All target objectives are met but with a slightly increased dose in the inter-phase junction compared to Figure (a) (red arrow). (d) Dose distribution EQD2-corrected, showing improved dose coverage in the inter-phase junction compared to Figure (b) (red arrow). *Figure from Paper I.*

Control of the inter-phase junction was applied, and CBCT positioning data revealed that 21 out of 815 fractions with CBCT imaging showed weekly longitudinal shifts greater than 4 mm. Two patients had three image fractions with shifts greater than 4 mm, four patients had two such fractions, and seven patients had one. The maximum longitudinal shift observed during a single fraction was 6.5 mm.

Planned versus estimated delivered dose

The registration performed between the planning CT and weekly CBCTs for seven CBCT studies for each responder and ten for each non-responder resulted in 868 registrations. The median vDSC for the rectum was 0.89 (IQR 0.86–0.90), and for the bladder, it was 0.93 (IQR 0.93–0.95).

Differences in dose-volume metrics between the planned and estimated delivered doses for the examined OARs were generally modest, although statistically significant (Table 2).

Table 2. Comparison between selected planned and estimated dose-volume metrics for the rectum, anal canal, bladder and bladder trigone. P-values < 0.05 were considered statistically significant. *Table adapted from Paper III.*

OARs Median vol. (IQR)		**All patients** n 97						
Rectum 74.4cc (65.1—88.9)		**Planned dose-volume**	Median ±95% CI	**Delivered dose-volume**	Median ±95% CI	**Median difference ***	Median ±95% CI	**p value**
$D_{2\%}$	(Gy)	**72.0**	71.6 — 72.3	**71.7**	71.1 — 71.9	**-0.4**	-0.5 — -0.3	**< 0.001**
V_{50Gy}	(%)	**38.2**	37.0 — 39.6	**37.7**	35.3 — 40.1	**0.1**	-0.9 — 1.1	0.79
V_{60Gy}	(%)	**30.7**	28.7 — 31.7	**28.7**	26.1 — 31.0	**-1.1**	-2.3 — -0.1	**0.025**
V_{65Gy}	(%)	**26.3**	24.1 — 27.4	**23.2**	21.3 — 25.6	**-2.0**	-3.2 — -0.9	**< 0.001**
V_{70Gy}	(%)	**14.8**	13.1 — 17.2	**11.5**	9.5 — 14.7	**-2.4**	-3.4 — -1.7	**< 0.001**
AnalCanal 11.2cc (9.1—15.0)		**Planned dose-volume**	Median ±95% CI	**Delivered dose-volume**	Median ±95% CI	**Median difference ***	Median ±95% CI	**p value**
$D_{2\%}$	(Gy)	**71.2**	70.9 — 71.5	**70.9**	70.6 — 71.0	**-0.5**	-0.7 — -0.3	**< 0.001**
V_{50Gy}	(%)	**23.9**	19.7 — 28.2	**25.4**	21.6 — 28.4	**0.3**	-1.1 — 1.9	0.71
V_{60Gy}	(%)	**18.4**	14.4 — 21.8	**18.2**	15.9 — 21.8	**-0.5**	-1.7 — 0.7	0.43
V_{65Gy}	(%)	**15.3**	12.1 — 18.6	**14.6**	11.9 — 17.5	**-0.9**	-2.0 — 0.1	0.096
V_{70Gy}	(%)	**8.8**	6.1 — 10.9	**5.9**	4.8 — 8.4	**-1.3**	-2.0 — -0.7	**< 0.001**
Bladder 80.8cc (59.2—131.8)		**Planned dose-volume**	Median ±95% CI	**Delivered dose-volume**	Median ±95% CI	**Median difference ***	Median ±95% CI	**p value**
D_{mean}	(Gy)	**61.9**	58.4 — 64.5	**62.4**	59.2 — 63.6	**0.2**	-0.8 — 1.3	0.73
$D_{2\%}$	(Gy)	**73.3**	72.9 — 73.6	**72.2**	72.0 — 72.6	**-0.8**	-0.9 — -0.7	**< 0.001**
V_{65Gy}	(%)	**69.1**	59.8 — 74.1	**57.4**	52.5 — 65.3	**-5.0**	-7.5 — -2.5	**< 0.001**
V_{70Gy}	(%)	**48.2**	42.8 — 57.8	**38.8**	34.4 — 45.0	**-8.4**	-11.1 — -6.1	**< 0.001**
Bladder Trigone 8.6cc (7.3—10.5)		**Planned dose-volume**	Median ±95% CI	**Delivered dose-volume**	Median ±95% CI	**Median difference ***	Median ±95% CI	**p value**
D_{mean}	(Gy)	**71.2**	70.3 — 71.6	**70.8**	70.0 — 71.1	**-0.2**	-0.4 — -0.1	**< 0.001**
$D_{2\%}$	(Gy)	**73.1**	72.4 — 73.8	**72.4**	72.0 — 72.8	**-0.6**	-0.8 — -0.5	**< 0.001**
V_{65Gy}	(%)	**100,0**	100.0 — 100.0	**100.0**	99.8 — 100.0	**-0.1**	-0.9 — 0.0	**0.0021**
V_{70Gy}	(%)	**98.3**	81.4 — 100.0	**86.7**	73.4 — 95.7	**-4.4**	-6.4 — -2.0	**< 0.001**

*Hodges-Lehman median difference

We found significant associations between dose-volume constraints recommended by QUANTEC and acute bowel toxicity grade ≥ 2, as well as late patient-reported urinary symptoms, $PROM_{10\%}$, for both the planned and estimated delivered dose distributions.

Ultra-hypofractionated simultaneous integrated boost, including seminal vesicles (Paper IV)

Dose-volume histogram (DVH) metrics for target volumes and OARs were evaluated using EQD2 (α/β=3 Gy) corrected dose distributions. These metrics were derived from the physical dose-volume objectives/constraints employed in our clinic for CF (78.0 Gy in 39 fractions), which are based on the QUANTEC criteria [109, 110].

All OAR dose metrics, except near maximum doses, were statistically significantly lower for UHF-SIB compared to CF sequential boost for elective and definite SV treatment. Figure 8a-c shows average DVH in EQD2 for the rectum, bladder, and bladder trigone for the UHF-SIB(α/β/=3), CF sequential boost, and UHF prostate-only plans.

The QUANTEC-based dose-volume criteria show that the median rectum and bladder doses are 2-7% and 2-4% lower, respectively, in the UHF-SIB as compared to CF treatment planning. The D98% to elective SV is 7-12Gy3 lower with UHF-SIB, and the corresponding data for verified SV is about 2-3Gy3 lower as compared to CF. For prostate-only treatments (42.7Gy), the SV(10mm) V90%/(29.5Gy) for CTV/PTV is in median (IQR) 99% (87-100)/78% (58-99) (Paper IV).

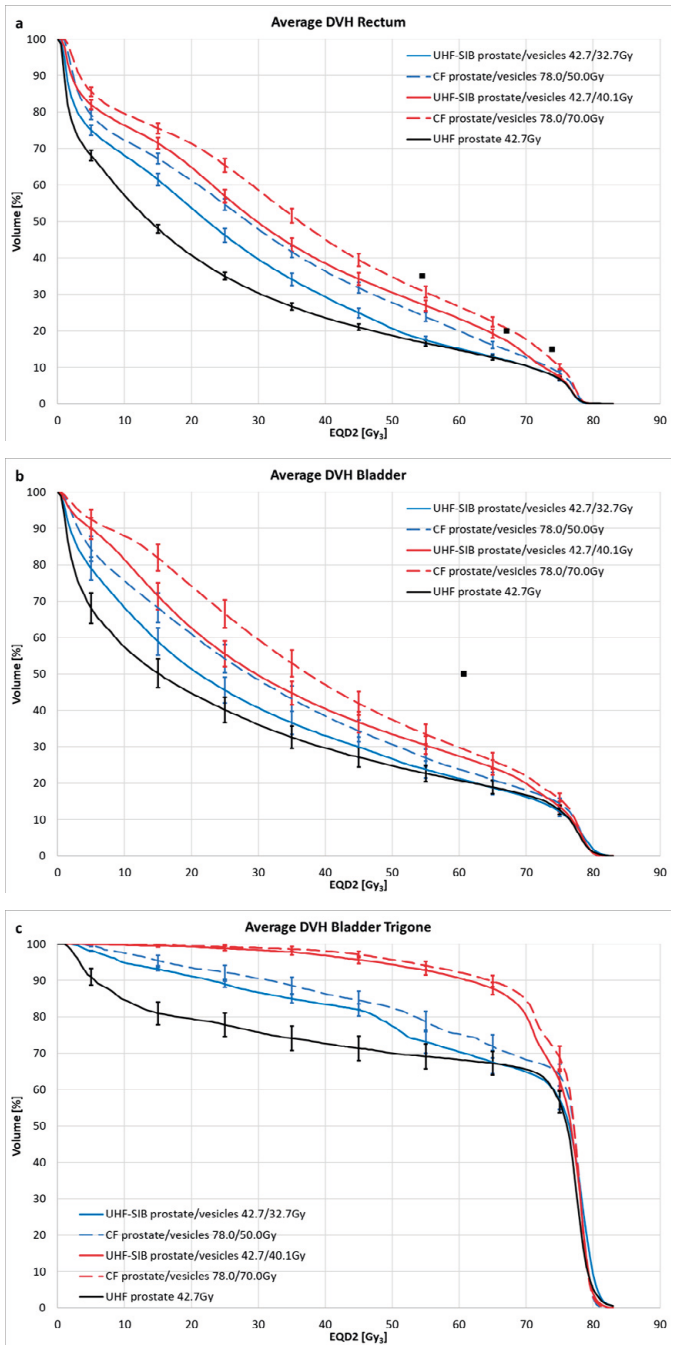

Figure 8. Average dose-volume-histograms and standard error in EQD2(α/β=3) for the UHF-SIB(α/β=3), CF sequential boost and UHF prostate-only dose plans for (a) rectum, (b) bladder and (c) bladder trigone. Squares indicate evaluated QUANTEC dose-volume criteria for the rectum and bladder. *Figure from Paper IV.*

General discussion and future perspectives

Since the initiation of this thesis, a new adaptive treatment planning approach for patients with PSA recurrence after prostatectomy has been developed. It has been tested in a phase II trial and implemented in an ongoing phase III program. The robustness of estimating planned versus estimated delivered doses to OARs has been compared and correlated to treatment toxicity. Finally, an analysis of delivering a simultaneous integrated boost to the seminal vesicles with UHF has been performed and further included in a prospective phase II trial.

Papers I-III

It has been eight years since the PROPER 1 study opened for inclusion. The last patient was enrolled five years ago (Papers I-II). During this time, we have introduced and further developed a treatment planning method with the aim of personalising treatment for patients with prostate cancer recurrence. The plan-on-plan technique used in our set-up has previously been used to optimise treatment plans [111, 112], but not to adapt treatment during the course of radiotherapy as done in PROPER 1. Therefore, to the best of our knowledge, this approach is unique. The clinical results from the PROPER 1 trial support that this method of delivering salvage radiotherapy seems safe and effective, with a high FFS rate among non-responders and moderate side effects. The low rate of treatment failure observed for SRT responders who received local SRT is consistent with the findings of our previous PSA study. The comparison of non-responders without PLNRT with a matched cohort of 152 patients from the same study, using the same definition of responder/non-responder and median follow-up time, demonstrated a 37% FFS rate at three years in the former group, as opposed to the 68% FFS rate observed in the non-responder group treated with PLNRT in the PROPER 1 study (Figure 9). These results indicate that PSA non-response during SRT for the prostate bed is frequently associated with lymph node metastases and that radiotherapy can effectively treat these metastases.

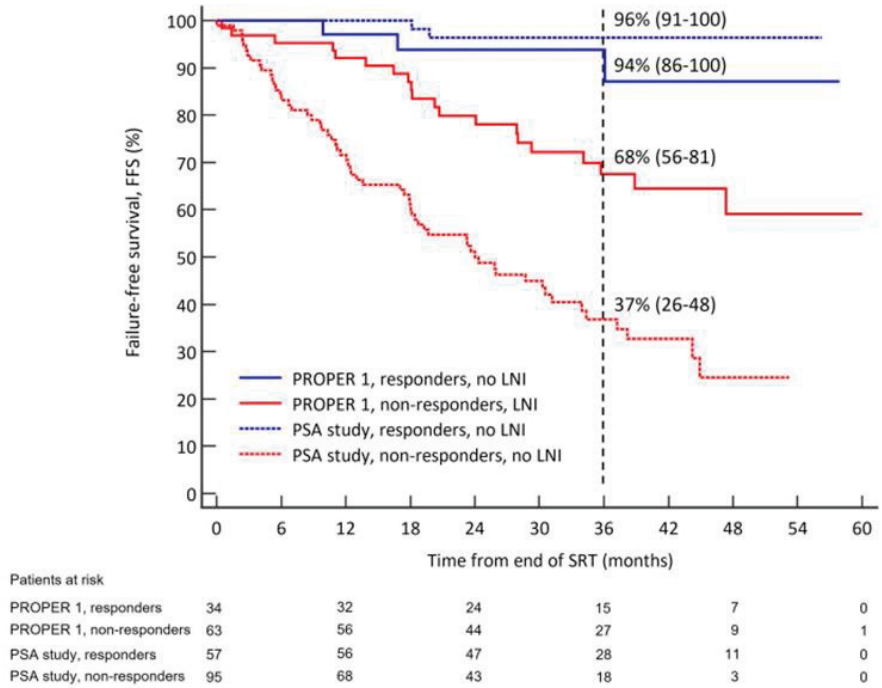

Figure 9. Failure-free survival of responders and non-responders in the PROPER 1 study and a matched cohort of 152 patients from the PSA study. Failure-free survival at three years is given with corresponding interquartile ranges. *Figure from supplementary Paper II.*

The sequential plan-on-plan treatment planning method was improved through continuous testing and refinement to enhance target coverage. By EQD2-correcting the base plan and implementing plan-on-plan optimisation, we delivered higher doses to the inter-phase junction, where target coverage was slightly limited during the first phase of the PROPER 1 study. This innovation has laid the foundation for our ongoing prospective phase III trial, PROPER 2, which started including patients in 2021. The PROPER 2 study aims to confirm the clinical benefits of this treatment approach.

Treating PET-positive local recurrence(s) when 50 Gy of 70 Gy is already given to the prostate bed is a challenge. This was accomplished by giving 2.3 - 2.5 Gy per fraction with the SIB technique to the local recurrence(s) volumes, equivalent to a total dose of 74 Gy - 78 Gy $EQD2_{\alpha/\beta=3}$ (Figures 10 and 11). If the local recurrence(s) was close to critical risk organs, the dose was reduced to 74 Gy $EQD2_{\alpha/\beta=3}$ for safety reasons, which is considered a sufficient dose level in the primary treatment setting [28]. However, the results from the PSMA-PET will be available already at baseline for future patients, and thereby, it will be possible to start with higher SIB doses to

the local recurrence already at the start of SRT as is done in the ongoing PROPER 2 trial (see above).

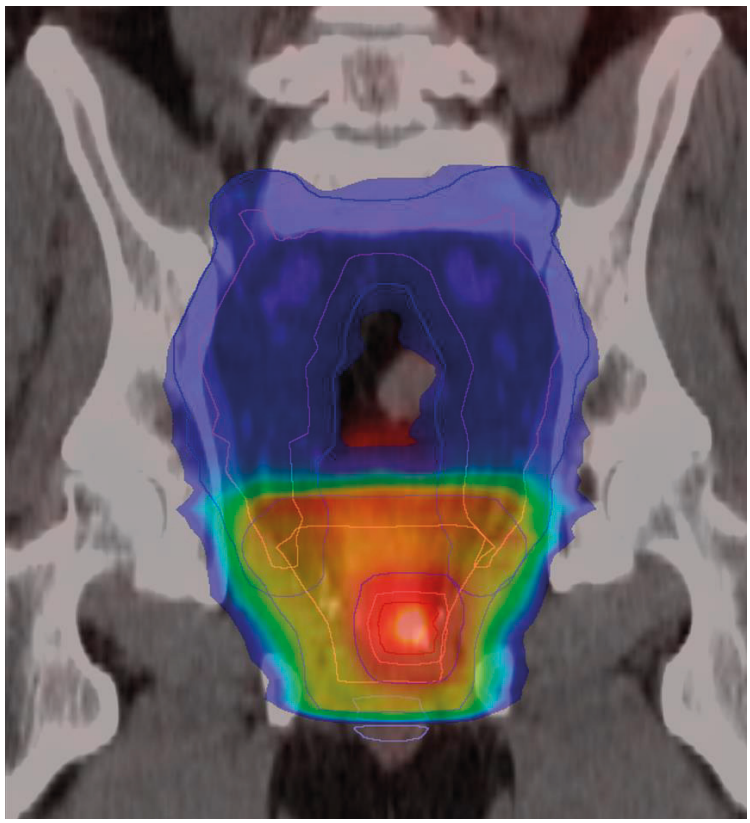

Figure 10. Dose summary in colour wash for a patient in the PROPER 1 study. 50 Gy to the pelvic lymph node (blue colour), 70 Gy to the prostate bed (green-yellow colour) and 78 Gy EQD2 $_{\alpha/\beta=3}$ to ^{68}Ga-PSMA-PET positive local recurrence (red colour). *©Vilberg Jóhannesson*

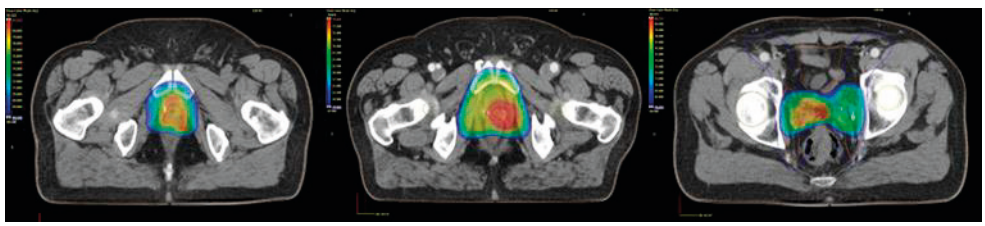

Figure 11. Three examples of local recurrences treated with SIB technique, 70 Gy to the prostate bed (green-yellow colour) and 74-78 Gy EQD2$_{\alpha/\beta=3}$ to local recurrence (red colour). *©Vilberg Jóhannesson*

Whether lymph node irradiation is beneficial for prostate cancer patients has been a matter of debate. Results from a randomised SRT trial, SPPORT [8], were recently presented where patients with biochemical recurrence were randomised to either prostate bed irradiation only, prostate bed irradiation only plus short hormonal therapy (ADT) or targeting both the prostate bed and PLNRT while combining it with short-term ADT. The results from SPPORT showed a significantly improved 5-year freedom from progression for both the addition of hormonal therapy only and hormonal therapy with PLNRT. No overall survival benefit was observed. Toxicity outcomes indicated significantly higher toxicity in the groups receiving ADT compared to the group without ADT and in the group getting PLNRT compared with the group without PLNRT. Notably, the benefit of PLNRT in this trial was not present at low PSA levels (below the median of 0.35 ng/ml). For this group of patients, it would be beneficial to identify further who would benefit from PLNRT.

Terlizzi and Bossi discussed whether all patients would be offered PLNRT [113]. They stated, "pelvic RT should be offered to all patients in the salvage setting in combination with short-term ADT". In contrast, they also pointed out that patients with BCR are a heterogeneous group and that some patients with favourable features may be spared from both ADT and PLNRT. The latter observation aligns with the outcome observed in the PROPER 1 study, which will be further validated through our phase 3 trial, PROPER 2. With the PROPER approach, a considerable proportion of the patients can potentially be spared from undergoing needless extended radiotherapy and unnecessary ADT, thereby reducing the side effects of the treatment. Further, our method could benefit patients with other tumour types with a biomarker comparable to PSA available to predict treatment outcomes.

The detection rate of PSMA-PET in the study cohort was slightly lower than anticipated for patients with comparable PSA levels [68]. A notable difference in detection rates was observed between the responder group (9%) and the non-responder group (35%), which was statistically significant. The trial served as a feasibility study for PSMA-PET imaging, and therefore, the PSMA-PET findings were not initially used for treatment planning or exclusion from curative treatment. According to our results, with several false positive findings in both the responder and non-responder group, excluding patients from curative treatment based on PSMA-PET results at low PSA levels should be done with precaution.

Radiotherapy treatment planning is traditionally based on a single planning CT study where the patient is scanned in the treatment position before the start of radiotherapy. It is well known that the anatomy can change both before treatment starts and during therapy [14, 15]. A more precise planning approach could be to adapt dose delivery according to these changes. Our results based on weekly CBCT scanning showed that such an approach would give significantly different doses to OARs. However, these differences were small in absolute terms. Our results were limited to only one CT scan per week, and it is possible that daily CBCTs would

discover even greater differences. Our findings differed somewhat between different OARs. For example, we found no significant differences in the mean dose to the bladder between planned and estimated delivered doses. In contrast, there were notable differences in the mean dose to the bladder trigone between planned and estimated delivered doses (although small in absolute terms). When considering side effects, we only found a correlation in acute GI toxicity regarding doctor´s scored RTOG toxicity and for more dose levels regarding estimated delivered compared to planned doses. Similarly, for patient-reported late side effects, we observed, for example, relationships between the planned and estimated delivered doses to the bladder and bladder trigone to GU symptoms.

The variation of these organs from planning CT to the start of radiotherapy and during therapy affects the dose distributions significantly, as shown in Figure 12. A proper bladder filling protocol and rectal preparations are essential to minimise these differences. Whether that is sufficient to make the dose-planning CT representative for the whole treatment and reduce differences between estimated and planned doses is not well known. Our results are in line with those of Buranaporn et al. [17], showing differences between estimated and planned doses. As present methods to evaluate dose during therapy are labour intensive, it is probably most important to improve bladder and bowel filling protocols to ensure accurate estimations of treatment outcomes. However, with future AI methods, daily adaptive treatment planning will likely further improve these estimations [114].

One example of how OARs are affected by bladder or bowel filling differences is the bladder trigone. Several publications address the function of the trigone [19, 25], and how it may play a significant role in GU side effects [20, 23, 26, 115]. During a radical prostatectomy, when the prostate is removed, the bladder base is attached to the pelvic floor. This stretches the bladder and, consequently, the bladder trigone, with parts that extend inside the target (CTV) during salvage radiotherapy after biochemical recurrence. In such cases, bladder filling also affects the extension of the trigone, as illustrated in Figure 12. The mean dose to the bladder decreases from almost 88% (empty bladder) of the dose to under 30% (full bladder), and the trigone's mean dose decreases from nearly 97% (empty bladder) to 77% (full bladder). Conversely, as seen in Figure 12d, the mean dose to the bladder increases from 20% to 90%, and the dose to the trigone rises from just over 60% to 100% of the prescribed dose.

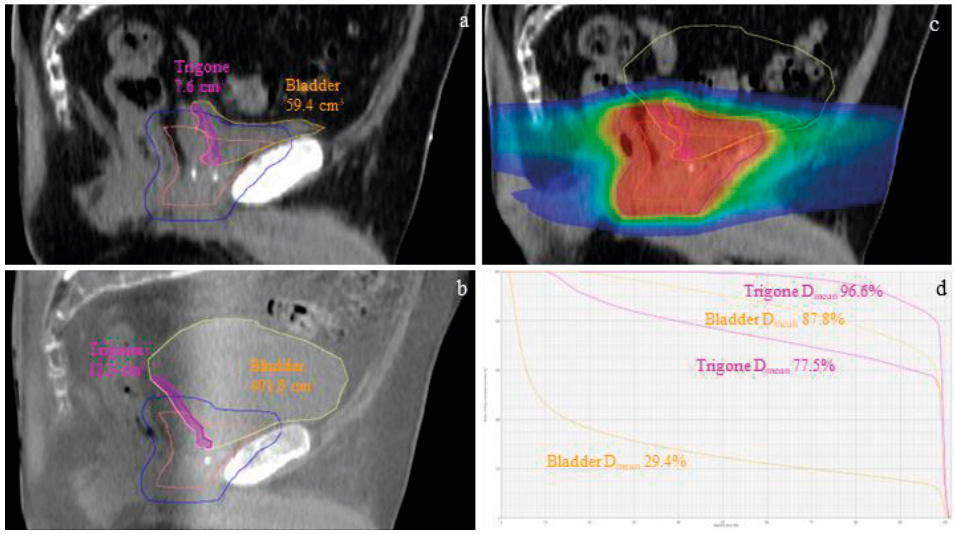

Figure 12. CT images from a patient in the PROPER 1 study; (a) preparation CT scan, (b) CBCT scan under treatment, (c) the dose distribution on the CT scan, and (d) dose-volume histogram (DVH) showing the bladder and bladder trigone doses. *©Vilberg Jóhannesson*

These results underscore the need to develop future, preferably AI-based methods to improve precision and efficiency in anatomical registrations. These methods should facilitate more accurate, rapid, and clinically meaningful dose-volume evaluations. Moreover, they should enable dose distribution adaptation based on bladder and rectum filling, potentially reducing doses to organs at risk. Such advancements would automatically retrieve dose-volume data, enhancing the accuracy of data generated during treatment.

Paper IV

Ultra-hypofractionation is being increasingly used in the treatment of localised prostate cancer in Sweden [64]. In the Scandinavian HYPO-RT-PC trial [32], the prostate gland was treated to 42.7 Gy in 7 fractions. No elective SV volumes were included in this trial. Therefore, patients with high-risk prostate cancer are most commonly treated with CF. By defining appropriate SV UHF doses, high-risk patients could benefit from receiving UHF with SV irradiation. When evaluating the possibility of increasing the fractionation doses for seminal vesicles while delivering ultra-hypofractionation RT to the prostate using a SIB technique, lower doses to organs at risk (OARs) were observed with UHF-SIB as compared to the CF sequential boost technique. This finding is consistent with observations for other diagnoses, such as head and neck cancer, anal cancer, and cervical cancer, where

transitioning from the sequential boost technique to the SIB technique in clinical practice has resulted in reductions in OAR doses [116-119].

Treatment planning with the SIB technique was performed with adequate dose coverage of the prostate and all elective target volumes (10 and 20 mm of the SV (31.2 $Gy_{\alpha/\beta=2}$ and 32.7 $Gy_{\alpha/\beta=3}$) or dose to 10 and 20 mm of verified SVI, (37.8 $Gy_{\alpha/\beta=2}$ and 40.1 $Gy_{\alpha/\beta=3}$)) (Figure 13). This UHF-SIB technique brings the dose to SV closer to the prescribed dose than the CF sequential boost technique. With the sequential technique, an extra dose is delivered to the SV when treating the prostate only.

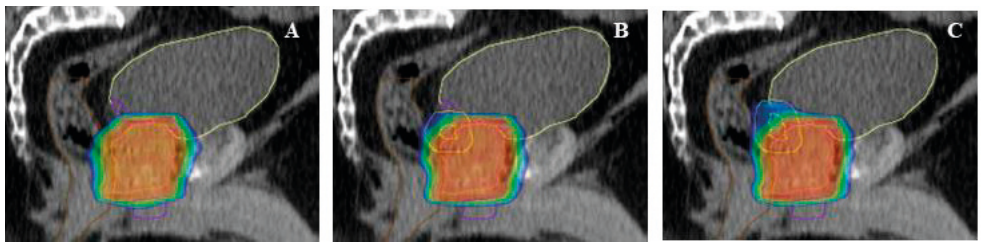

Figure 13. Dose distribution in color wash (sagittal view); (A) prostate, (B) prostate and 10mm seminal vesicles and (C) prostate and 20mm seminal vesicles. *©Vilberg Jóhannesson*

This study aimed to identify a treatment planning approach to implement UHF-SIB-SV clinically in high-risk prostate cancer patients. This has been accomplished in a new trial called the HYPO-RT-PC-boost (NCT06220435), which includes not only the seminal vesicles but also pelvic lymph nodes and incorporates boosts to MRI-identified focal tumour lesions. This trial utilises the UHF-SIB technique with the elective SV doses described in our work.

Conclusions

Altogether, this thesis has contributed to developing and exploring new radiotherapy treatment planning methods for prostate cancer patients. The following are the primary conclusions that can be drawn from the studies presented in this thesis:

- Sequential VMAT treatment planning can achieve good target coverage and acceptable doses to the OARs through biologically adaptive plan-on-plan optimisation (Paper I).
- The intensified SRT resulted in high failure-free survival rates among non-responders with moderate side effects, indicating a clinically significant impact of selective PLNRT on a patient group with a poor prognosis according to PSA response (Paper II).
- PSMA-PET findings seem rare in treatment responders, and the occurrence of false positive findings, even for non-responders, warrants caution in the guidance of treatment intention for these patients based on PET findings (Paper II).
- Small differences were observed between the planned and estimated delivered dose distributions upon evaluation with weekly CBCTs in the PROPER 1 trial (Paper III).
- There was an increasing trend toward a stronger association with side effects for specific estimated metrics of rectal, bladder, bladder trigone, and anal canal doses, as compared to planned doses (Paper III).
- Ultra-hypofractionated radiotherapy with a SIB technique to the prostate and seminal vesicles can be planned with generally lower doses (EQD2) to organs at risk, compared to conventionally fractionated radiotherapy based on a sequential boost technique (Paper IV).

To summarise, the practical implications of this thesis enable advanced radiation planning techniques for optimising VMAT for primary and recurrent prostate cancer. The resulting individualised adapted radiotherapy may improve the treatment outcomes with lower side effects.

Acknowledgements

There are many who have inspired, supported, and contributed to the development of this thesis, I would like to express my gratitude to all of you.

To my main supervisor, **Aðalsteinn Gunnlaugsson**, for taking me with you on this study journey that started more than ten years ago. Also, thank you for all the runs in Skrylle and Häckeberga, where the studies were discussed and the ideas for my theses came forward. Thanks for the inspiration and for all the support. You are a dear friend to have.

To my co-supervisor, **Elinore Wieslander**, for your never-ending enthusiasm and support during the process. I appreciate you sharing, your expertise and inspiration.

To my co-supervisor and boss **Sven Bäck**, my sincere gratitude for your devotion and concern throughout my work.

To my expert supervisor, **Per Nilsson**, thank you for being an amplifier and a great inspiration. You are solid as a ROCK!

To my expert supervisor, **Elisabeth Kjellén**, thank you for your encouragement and precision comments, spot-on!

To my dear colleagues in the radiotherapy treatment planning group in Lund during my research time:
Alla Nilsson, Caisa Kjellström, Carina Andersson Ljus, Felix Månsson, Hedda Enocson, Ingrid Kristensen, Joanie Guei, Joakim Nilsson, Kristina Hallberg, Lovisa Berg, Mahnaz Haghanegi, Malin Hedetoft, Marie Tärnhuvud, Mizgin Coskun, Niklas Svanberg, Pia Frederiksen, Rebecka Ericsson Szecsenyi, Sara Falk, Sara Talozi, Sotirios Mouras, Victor Pham and **Viktor Rogowski.**
Thank you all for your concern and support**.**

I sincerely thank **Silke Engelholm** and **Per Munck af Rosenschöld** for enabling me to combine clinical work and research.

The valuable co-authors of the PROPER 1 study**, Eva Brun, Ulrika Bitzén, Göran Ahlgren, Tomas Olsson, Ola Bratt**, **Olof Ståhl** and **Patrik Brynolfsson** thank you for the collaboration and your inspiring work with the manuscripts.

To all of you at the **radiotherapy department** and the **radiotherapy physics department** in Lund, there are many of you who have inspired and supported me during the time of the work – thank you so much.

Team Iceland, **Dröfn** og **Steini**, **Dóra** og **Frikki**, **Jón Örn** og **Nína**, thank you for all the visits and wonderful recreational activities together!

My brother-in-law – Kæri **Jón Páll** og fjölskylda, þið eruð frábær, takk fyrir allar heimsóknir.

My sisters – Elsku **Hulda, Bidda** og fjölskyldur, takk fyrir allan kærleik og samverustundir.

My parents-in-law – Elsku **Magga** og **Tani**, hjartans þakkir fyrir allan stuðning og velvild i gegnum árin, alveg ómetanlegt að eiga góðan bakhjarl hjá ykkur.

My parents, **Guðrún** og **Jóhannes** – Elsku mamma og pabbi, hjartans þakkir fyrir ad vera mér góð fyrirmynd og stappad stálinu í mig þegar þess þurfti. Er ykkur afar þakklátur fyrir allan stuðning og kærleika. Elsku mamma, án þín hefði ég aldrei fengið þá hugmynd að verða Geislafræðingur og þar með sennilega ekki verið í þessum sporum í dag.

Amor, the dog, a great companion at the home office.

My wonderful children, **Valgerður Margrét, Andrés** og **Rannveig Edda** thanks for your love and understanding during my PhD work.

My dear wife, **Anna María** thanks for being my role model and supporting me through my studies, I couldn't have done this without you. I love U ♥

In memory of Professor **Peter Höglund**, who supported and helped me in the early stages of my PhD studies. Peter passed away suffering from prostate cancer in September 2019.

References

1. Paz-Manrique R, Morton G, Vera FQ, Paz-Manrique S, Espinoza-Briones A, Deza CM. Radiation therapy after radical surgery in prostate cancer. Ecancermedicalscience. 2023;17:1565 https://doi.org/10.3332/ecancer.2023.1565.
2. Beckmann K, Garmo H, Nilsson P, Franck Lissbrant I, Widmark A, Stattin P. Radical radiotherapy for prostate cancer: patterns of care in Sweden 1998-2016. Acta Oncol. 2020;59(5):549-57 https://doi.org/10.1080/0284186x.2020.1730003.
3. Varian medical systems. Eclipse Photon and Electron Reference Guide 2017 [MyVarian; 245-6]. https://www.myvarian.com/s/login/?ec=302&startURL=%2Fs%2F.
4. Shahabi A, Satkunasivam R, Gill IS, Lieskovsky G, Daneshmand S, Pinski JK, et al. Predictors of time to biochemical recurrence in a radical prostatectomy cohort within the PSA-era. Can Urol Assoc J. 2016;10(1-2):E17-22 https://doi.org/10.5489/cuaj.3163.
5. Chang JH, Park W, Park JS, Pyo H, Huh SJ, Choi HY, et al. Significance of early prostate-specific antigen values after salvage radiotherapy in recurrent prostate cancer patients treated with surgery. Int J Urol. 2015;22(1):82-7 https://doi.org/10.1111/iju.12604.
6. King CR. The dose-response of salvage radiotherapy following radical prostatectomy: A systematic review and meta-analysis. Radiother Oncol. 2016;121(2):199-203 https://doi.org/10.1016/j.radonc.2016.10.026.
7. Stephenson AJ, Scardino PT, Kattan MW, Pisansky TM, Slawin KM, Klein EA, et al. Predicting the outcome of salvage radiation therapy for recurrent prostate cancer after radical prostatectomy. J Clin Oncol. 2007;25(15):2035-41 https://doi.org/10.1200/jco.2006.08.9607.
8. Pollack A, Karrison TG, Balogh AG, Gomella LG, Low DA, Bruner DW, et al. The addition of androgen deprivation therapy and pelvic lymph node treatment to prostate bed salvage radiotherapy (NRG Oncology/RTOG 0534 SPPORT): an international, multicentre, randomised phase 3 trial. Lancet. 2022;399(10338):1886-901 https://doi.org/10.1016/s0140-6736(21)01790-6.
9. Afshar-Oromieh A, Malcher A, Eder M, Eisenhut M, Linhart HG, Hadaschik BA, et al. PET imaging with a [68Ga]gallium-labelled PSMA ligand for the diagnosis of prostate cancer: biodistribution in humans and first evaluation of tumour lesions. Eur J Nucl Med Mol Imaging. 2013;40(4):486-95 https://doi.org/10.1007/s00259-012-2298-2.

10. Afshar-Oromieh A, Avtzi E, Giesel FL, Holland-Letz T, Linhart HG, Eder M, et al. The diagnostic value of PET/CT imaging with the (68)Ga-labelled PSMA ligand HBED-CC in the diagnosis of recurrent prostate cancer. Eur J Nucl Med Mol Imaging. 2015;42(2):197-209 https://doi.org/10.1007/s00259-014-2949-6.
11. Afshar-Oromieh A, Hetzheim H, Kratochwil C, Benesova M, Eder M, Neels OC, et al. The Theranostic PSMA Ligand PSMA-617 in the Diagnosis of Prostate Cancer by PET/CT: Biodistribution in Humans, Radiation Dosimetry, and First Evaluation of Tumor Lesions. J Nucl Med. 2015;56(11):1697-705 https://doi.org/10.2967/jnumed.115.161299.
12. Afshar-Oromieh A, Zechmann CM, Malcher A, Eder M, Eisenhut M, Linhart HG, et al. Comparison of PET imaging with a (68)Ga-labelled PSMA ligand and (18)F-choline-based PET/CT for the diagnosis of recurrent prostate cancer. Eur J Nucl Med Mol Imaging. 2014;41(1):11-20 https://doi.org/10.1007/s00259-013-2525-5.
13. Thor M, Bentzen L, Hysing LB, Ekanger C, Helle SI, Karlsdóttir Á, et al. Prediction of rectum and bladder morbidity following radiotherapy of prostate cancer based on motion-inclusive dose distributions. Radiother Oncol. 2013;107(2):147-52 https://doi.org/10.1016/j.radonc.2013.03.029.
14. Akin M, Öksüz DC, Iktueren B, Ambarcioglu P, Karacam S, Koca S, et al. Does rectum and bladder dose vary during the course of image-guided radiotherapy in the postprostatectomy setting? Tumori. 2014;100(5):529-35 https://doi.org/10.1700/1660.18172.
15. Grün A, Kawgan-Kagan M, Kaul D, Badakhshi H, Stromberger C, Budach V, et al. Impact of bladder volume on acute genitourinary toxicity in intensity modulated radiotherapy for localized and locally advanced prostate cancer. Strahlenther Onkol. 2019;195(6):517-25 https://doi.org/10.1007/s00066-018-1398-8.
16. Oh S, Kim S. Deformable image registration in radiation therapy. Radiat Oncol J. 2017;35(2):101-11 https://doi.org/10.3857/roj.2017.00325.
17. Buranaporn P, Dankulchai P, Jaikuna T, Prasartseree T. Relation between DIR recalculated dose based CBCT and GI and GU toxicity in postoperative prostate cancer patients treated with VMAT. Radiother Oncol. 2021;157:8-14 https://doi.org/10.1016/j.radonc.2020.12.036.
18. Andersen ES, Muren LP, Sørensen TS, Noe KO, Thor M, Petersen JB, et al. Bladder dose accumulation based on a biomechanical deformable image registration algorithm in volumetric modulated arc therapy for prostate cancer. Phys Med Biol. 2012;57(21):7089-100 https://doi.org/10.1088/0031-9155/57/21/7089.
19. Woodburne RT. THE URETER, URETEROVESICAL JUNCTION, AND VESICAL TRIGONE. Anat Rec. 1965;151:243 https://doi.org/10.1002/ar.1091510305.
20. Henderson DR, Murray JR, Gulliford SL, Tree AC, Harrington KJ, Van As NJ. An Investigation of Dosimetric Correlates of Acute Toxicity in Prostate Stereotactic Body Radiotherapy: Dose to Urinary Trigone is Associated with Acute Urinary Toxicity. Clin Oncol (R Coll Radiol). 2018;30(9):539-47 https://doi.org/10.1016/j.clon.2018.05.001.

21. Park JH, Kim YS, Park J, Ahn H, Kim CS, Kim M, et al. Incidence and dose-volume analysis of acute bladder toxicity following pelvic radiotherapy. Tumori. 2014;100(2):195-200 https://doi.org/10.1177/030089161410000213.
22. Harsolia A, Vargas C, Yan D, Brabbins D, Lockman D, Liang J, et al. Predictors for chronic urinary toxicity after the treatment of prostate cancer with adaptive three-dimensional conformal radiotherapy: dose-volume analysis of a phase II dose-escalation study. Int J Radiat Oncol Biol Phys. 2007;69(4):1100-9 https://doi.org/10.1016/j.ijrobp.2007.04.076.
23. Mylona E, Ebert M, Kennedy A, Joseph D, Denham J, Steigler A, et al. Rectal and Urethro-Vesical Subregions for Toxicity Prediction After Prostate Cancer Radiation Therapy: Validation of Voxel-Based Models in an Independent Population. Int J Radiat Oncol Biol Phys. 2020;108(5):1189-95 https://doi.org/10.1016/j.ijrobp.2020.07.019.
24. Dobberfuhl AD, van Uem S, Versi E. Trigone as a diagnostic and therapeutic target for bladder-centric interstitial cystitis/bladder pain syndrome. Int Urogynecol J. 2021;32(12):3105-11 https://doi.org/10.1007/s00192-021-04878-9.
25. Roosen A, Wu C, Sui G, Chowdhury RA, Patel PM, Fry CH. Characteristics of spontaneous activity in the bladder trigone. Eur Urol. 2009;56(2):346-53 https://doi.org/10.1016/j.eururo.2008.06.048.
26. Ghadjar P, Zelefsky MJ, Spratt DE, Munck af Rosenschöld P, Oh JH, Hunt M, et al. Impact of dose to the bladder trigone on long-term urinary function after high-dose intensity modulated radiation therapy for localized prostate cancer. Int J Radiat Oncol Biol Phys. 2014;88(2):339-44 https://doi.org/10.1016/j.ijrobp.2013.10.042.
27. Vogelius IR, Bentzen SM. Diminishing Returns From Ultrahypofractionated Radiation Therapy for Prostate Cancer. Int J Radiat Oncol Biol Phys. 2020;107(2):299-304 https://doi.org/10.1016/j.ijrobp.2020.01.010.
28. Dearnaley D, Syndikus I, Mossop H, Khoo V, Birtle A, Bloomfield D, et al. Conventional versus hypofractionated high-dose intensity-modulated radiotherapy for prostate cancer: 5-year outcomes of the randomised, non-inferiority, phase 3 CHHiP trial. Lancet Oncol. 2016;17(8):1047-60 https://doi.org/10.1016/s1470-2045(16)30102-4.
29. Incrocci L, Wortel RC, Alemayehu WG, Aluwini S, Schimmel E, Krol S, et al. Hypofractionated versus conventionally fractionated radiotherapy for patients with localised prostate cancer (HYPRO): final efficacy results from a randomised, multicentre, open-label, phase 3 trial. Lancet Oncol. 2016;17(8):1061-9 https://doi.org/10.1016/s1470-2045(16)30070-5.
30. Catton CN, Lukka H, Gu CS, Martin JM, Supiot S, Chung PWM, et al. Randomized Trial of a Hypofractionated Radiation Regimen for the Treatment of Localized Prostate Cancer. J Clin Oncol. 2017;35(17):1884-90 https://doi.org/10.1200/jco.2016.71.7397.
31. Lee WR, Dignam JJ, Amin MB, Bruner DW, Low D, Swanson GP, et al. Randomized Phase III Noninferiority Study Comparing Two Radiotherapy Fractionation Schedules in Patients With Low-Risk Prostate Cancer. J Clin Oncol. 2016;34(20):2325-32 https://doi.org/10.1200/jco.2016.67.0448.

32. Widmark A, Gunnlaugsson A, Beckman L, Thellenberg-Karlsson C, Hoyer M, Lagerlund M, et al. Ultra-hypofractionated versus conventionally fractionated radiotherapy for prostate cancer: 5-year outcomes of the HYPO-RT-PC randomised, non-inferiority, phase 3 trial. Lancet. 2019;394(10196):385-95 https://doi.org/10.1016/s0140-6736(19)31131-6.
33. Tree AC, Ostler P, van der Voet H, Chu W, Loblaw A, Ford D, et al. Intensity-modulated radiotherapy versus stereotactic body radiotherapy for prostate cancer (PACE-B): 2-year toxicity results from an open-label, randomised, phase 3, non-inferiority trial. Lancet Oncol. 2022;23(10):1308-20 https://doi.org/10.1016/s1470-2045(22)00517-4.
34. Salembier C, Villeirs G, De Bari B, Hoskin P, Pieters BR, Van Vulpen M, et al. ESTRO ACROP consensus guideline on CT- and MRI-based target volume delineation for primary radiation therapy of localized prostate cancer. Radiother Oncol. 2018;127(1):49-61 https://doi.org/10.1016/j.radonc.2018.01.014.
35. Thwaites DI, Tuohy JB. Back to the future: the history and development of the clinical linear accelerator. Physics in Medicine & Biology. 2006;51(13):R343 https://doi.org/10.1088/0031-9155/51/13/R20.
36. Van Dyk J, Battista J, Almond P. A Retrospective of Cobalt-60 radiation therapy : "The Atom Bomb that Saves Lives". 2020:2020.
37. Brahme A, Roos JE, Lax I. Solution of an integral equation encountered in rotation therapy. Phys Med Biol. 1982;27(10):1221-9 https://doi.org/10.1088/0031-9155/27/10/002.
38. Brahme A. Optimization of stationary and moving beam radiation therapy techniques. Radiother Oncol. 1988;12(2):129-40 https://doi.org/10.1016/0167-8140(88)90167-3.
39. Mackie TR. History of tomotherapy. Phys Med Biol. 2006;51(13):R427-53 https://doi.org/10.1088/0031-9155/51/13/r24.
40. Ling CC, Burman C, Chui CS, Kutcher GJ, Leibel SA, LoSasso T, et al. Conformal radiation treatment of prostate cancer using inversely-planned intensity-modulated photon beams produced with dynamic multileaf collimation. Int J Radiat Oncol Biol Phys. 1996;35(4):721-30 https://doi.org/10.1016/0360-3016(96)00174-5.
41. Otto K. Volumetric modulated arc therapy: IMRT in a single gantry arc. Med Phys. 2008;35(1):310-7 https://doi.org/10.1118/1.2818738.
42. Holt A, Van Gestel D, Arends MP, Korevaar EW, Schuring D, Kunze-Busch MC, et al. Multi-institutional comparison of volumetric modulated arc therapy vs. intensity-modulated radiation therapy for head-and-neck cancer: a planning study. Radiat Oncol. 2013;8:26 https://doi.org/10.1186/1748-717x-8-26.
43. Pusey D, Smith L, Zeman EM, Adams R. A history and overview of the certification exam for medical dosimetrists. Med Dosim. 2005;30(2):92-6 https://doi.org/10.1016/j.meddos.2005.03.001.
44. Tsien KC. The application of automatic computing machines to radiation treatment planning. Br J Radiol. 1955;28(332):432-9 https://doi.org/10.1259/0007-1285-28-332-432.

45. Haybittle JL, Houston AA. The use of a multi-access computer for radiation treatment planning. Br J Radiol. 1968;41(492):927-31 https://doi.org/10.1259/0007-1285-41-492-927.
46. Halldén H, Ragnhult I, Roos B. Computer Method for Treatment Planning in External Radiotherapy. Acta Radiologica: Therapy, Physics, Biology. 1963;1(6):407-16 https://doi.org/10.3109/02841866309134117.
47. Orr JS. Optimisation of radiotherapy treatment planning. Comput Programs Biomed. 1972;2(3):216-20 https://doi.org/10.1016/0010-468x(72)90031-1.
48. Hounsfield GN. Computerized transverse axial scanning (tomography): Part I. Description of system. 1973. Br J Radiol. 1995;68(815):H166-72
49. Pereira GC, Traughber M, Muzic RF, Jr. The role of imaging in radiation therapy planning: past, present, and future. Biomed Res Int. 2014;2014:231090 https://doi.org/10.1155/2014/231090.
50. Rockoff SD. The evolving role of computerized tomography in radiation oncology. Cancer. 1977;39(2 Suppl):694-6 https://doi.org/10.1002/1097-0142(197702)39:2.
51. Dobbs HJ, Parker RP, Hodson NJ, Hobday P, Husband JE. The use of CT in radiotherapy treatment planning. Radiother Oncol. 1983;1(2):133-41 https://doi.org/10.1016/s0167-8140(83)80016-4.
52. Stubbs J, Whitrow R. The three-dimensional display of the anatomy for radiotherapy treatment planning. Comput Biol Med. 1979;9(3):257-64 https://doi.org/10.1016/0010-4825(79)90009-x.
53. Kessler ML, Ten Haken RK, Fraass BA, McShan DL. Expanding the use and effectiveness of dose-volume histograms for 3-D treatment planning. I: Integration of 3-D dose-display. Int J Radiat Oncol Biol Phys. 1994;29(5):1125-31 https://doi.org/10.1016/0360-3016(94)90409-x.
54. Fraass BA. The development of conformal radiation therapy. Medical Physics. 1995;22(11):1911-21 https://doi.org/10.1118/1.597446.
55. Altschuler MD, Sontag MR, Bloch P. Rapid three-dimensional treatment planning: I. Ray-tracing approach to primary component dose calculations. Phys Med Biol. 1987;32(5):543-56 https://doi.org/10.1088/0031-9155/32/5/001.
56. Persson E, Jamtheim Gustafsson C, Ambolt P, Engelholm S, Ceberg S, Bäck S, et al. MR-PROTECT: Clinical feasibility of a prostate MRI-only radiotherapy treatment workflow and investigation of acceptance criteria. Radiat Oncol. 2020;15(1):77 https://doi.org/10.1186/s13014-020-01513-7.
57. Taylor A, Powell ME. Intensity-modulated radiotherapy--what is it? Cancer Imaging. 2004;4(2):68-73 https://doi.org/10.1102/1470-7330.2004.0003.
58. Samuelsson A, Johansson KA. Intensity modulated radiotherapy treatment planning for dynamic multileaf collimator delivery: influence of different parameters on dose distributions. Radiother Oncol. 2003;66(1):19-28 https://doi.org/10.1016/s0167-8140(02)00264-5.
59. Cho B. Intensity-modulated radiation therapy: a review with a physics perspective. Radiat Oncol J. 2018;36(1):1-10 https://doi.org/10.3857/roj.2018.00122.

60. Bucci MK, Bevan A, Roach M, 3rd. Advances in radiation therapy: conventional to 3D, to IMRT, to 4D, and beyond. CA Cancer J Clin. 2005;55(2):117-34 https://doi.org/10.3322/canjclin.55.2.117.
61. van Leeuwen CM, Oei AL, Crezee J, Bel A, Franken NAP, Stalpers LJA, et al. The alfa and beta of tumours: a review of parameters of the linear-quadratic model, derived from clinical radiotherapy studies. Radiat Oncol. 2018;13(1):96 https://doi.org/10.1186/s13014-018-1040-z.
62. Fowler JF. 21 years of biologically effective dose. Br J Radiol. 2010;83(991):554-68 https://doi.org/10.1259/bjr/31372149.
63. Nationella vårdprogrammet för prostatacancer. Version: 8.1 Regionala cancercentrum i samverkan. https://kunskapsbanken.cancercentrum.se/diagnoser/prostatacancer/vardprogram/.
64. NPCR Nationella prostatacancerregistret. https://npcr.se/rapporter/nationella-arsrapporter/.
65. Sedelaar JP, Vijverberg PL, De Reijke TM, de la Rosette JJ, Kil PJ, Braeckman JG, et al. Transrectal ultrasound in the diagnosis of prostate cancer: state of the art and perspectives. Eur Urol. 2001;40(3):275-84 https://doi.org/10.1159/000049787.
66. Mohsen N. Role of MRI, Ultrasound, and Computed Tomography in the Management of Prostate Cancer. PET Clin. 2022;17(4):565-83 https://doi.org/10.1016/j.cpet.2022.07.002.
67. van Leeuwen PJ, Stricker P, Hruby G, Kneebone A, Ting F, Thompson B, et al. (68) Ga-PSMA has a high detection rate of prostate cancer recurrence outside the prostatic fossa in patients being considered for salvage radiation treatment. BJU Int. 2016;117(5):732-9 https://doi.org/10.1111/bju.13397.
68. Perera M, Papa N, Roberts M, Williams M, Udovicich C, Vela I, et al. Gallium-68 Prostate-specific Membrane Antigen Positron Emission Tomography in Advanced Prostate Cancer-Updated Diagnostic Utility, Sensitivity, Specificity, and Distribution of Prostate-specific Membrane Antigen-avid Lesions: A Systematic Review and Meta-analysis. Eur Urol. 2020;77(4):403-17 https://doi.org/10.1016/j.eururo.2019.01.049.
69. Schwenck J, Rempp H, Reischl G, Kruck S, Stenzl A, Nikolaou K, et al. Comparison of (68)Ga-labelled PSMA-11 and (11)C-choline in the detection of prostate cancer metastases by PET/CT. Eur J Nucl Med Mol Imaging. 2017;44(1):92-101 https://doi.org/10.1007/s00259-016-3490-6.
70. Morigi JJ, Stricker PD, van Leeuwen PJ, Tang R, Ho B, Nguyen Q, et al. Prospective Comparison of 18F-Fluoromethylcholine Versus 68Ga-PSMA PET/CT in Prostate Cancer Patients Who Have Rising PSA After Curative Treatment and Are Being Considered for Targeted Therapy. J Nucl Med. 2015;56(8):1185-90 https://doi.org/10.2967/jnumed.115.160382.
71. Gleason DF. Histologic grading of prostate cancer: A perspective. Human Pathology. 1992;23(3):273-9 https://doi.org/10.1016/0046-8177(92)90108-F.
72. James D. Brierley (Editor) MKGE, Christian Wittekind (Editor). TNM Classification of Malignant Tumours, 8th Edition: Wiley-Blackwel; 2016.

73. Gomez-Iturriaga A, Büchser D, Miguel IS, Marban M, Urresola A, Ezquerro A, et al. MRI detected extaprostatic extension (EPE) in prostate cancer: Do all T3a patients have the same outcomes? Clin Transl Radiat Oncol. 2020;24:135-9 https://doi.org/10.1016/j.ctro.2020.08.002.
74. Lardas M, Liew M, van den Bergh RC, De Santis M, Bellmunt J, Van den Broeck T, et al. Quality of Life Outcomes after Primary Treatment for Clinically Localised Prostate Cancer: A Systematic Review. Eur Urol. 2017;72(6):869-85 https://doi.org/10.1016/j.eururo.2017.06.035.
75. van Poppel H, Everaerts W, Tosco L, Joniau S. Open and robotic radical prostatectomy. Asian J Urol. 2019;6(2):125-8 https://doi.org/10.1016/j.ajur.2018.12.002.
76. Siddiqui ZA, Krauss DJ. Adjuvant androgen deprivation therapy for prostate cancer treated with radiation therapy. Transl Androl Urol. 2018;7(3):378-89 https://doi.org/10.21037/tau.2018.01.06.
77. Brenner DJ. Fractionation and late rectal toxicity. International Journal of Radiation Oncology*Biology*Physics. 2004;60(4):1013-5 https://doi.org/10.1016/j.ijrobp.2004.04.014.
78. Dasu A, Toma-Dasu I. Prostate alpha/beta revisited – an analysis of clinical results from 14 168 patients. Acta Oncologica. 2012;51(8):963-74 https://doi.org/10.3109/0284186X.2012.719635.
79. Vogelius IR, Bentzen SM. Dose Response and Fractionation Sensitivity of Prostate Cancer After External Beam Radiation Therapy: A Meta-analysis of Randomized Trials. Int J Radiat Oncol Biol Phys. 2018;100(4):858-65 https://doi.org/10.1016/j.ijrobp.2017.12.011.
80. Zietman AL. Making Radiation Therapy for Prostate Cancer More Economical and More Convenient. Journal of Clinical Oncology. 2016;34(20):2323-4 https://doi.org/10.1200/jco.2016.67.3764.
81. Morgan SC, Hoffman K, Loblaw DA, Buyyounouski MK, Patton C, Barocas D, et al. Hypofractionated Radiation Therapy for Localized Prostate Cancer: An ASTRO, ASCO, and AUA Evidence-Based Guideline. Journal of Clinical Oncology. 2018;36(34):3411-30 https://doi.org/10.1200/jco.18.01097.
82. Cui M, Gao X-S, Li X, Ma M, Qi X, Shibamoto Y. Variability of α/β ratios for prostate cancer with the fractionation schedule: caution against using the linear-quadratic model for hypofractionated radiotherapy. Radiation Oncology. 2022;17(1):54 https://doi.org/10.1186/s13014-022-02010-9.
83. Ward JF, Blute ML, Slezak J, Bergstralh EJ, Zincke H. The Long-Term Clinical Impact of Biochemical Recurrence of Prostate Cancer 5 or More Years After Radical Prostatectomy. The Journal of Urology. 2003;170(5):1872-6 https://doi.org/10.1097/01.ju.0000091876.13656.2e.

84. Cookson MS, Aus G, Burnett AL, Canby-Hagino ED, D'Amico AV, Dmochowski RR, et al. Variation in the Definition of Biochemical Recurrence in Patients Treated for Localized Prostate Cancer: The American Urological Association Prostate Guidelines for Localized Prostate Cancer Update Panel Report and Recommendations for a Standard in the Reporting of Surgical Outcomes. The Journal of Urology. 2007;177(2):540-5 https://doi.org/10.1016/j.juro.2006.10.097.

85. Thompson IM, Valicenti RK, Albertsen P, Davis BJ, Goldenberg SL, Hahn C, et al. Adjuvant and Salvage Radiotherapy After Prostatectomy: AUA/ASTRO Guideline. The Journal of Urology. 2013;190(2):441-9 https://doi.org/10.1016/j.juro.2013.05.032.

86. Valicenti RK, Thompson I, Albertsen P, Davis BJ, Goldenberg SL, Wolf JS, et al. Adjuvant and Salvage Radiation Therapy After Prostatectomy: American Society for Radiation Oncology/American Urological Association Guidelines. International Journal of Radiation Oncology*Biology*Physics. 2013;86(5):822-8 https://doi.org/10.1016/j.ijrobp.2013.05.029.

87. Abugharib A, Jackson WC, Tumati V, Dess RT, Lee JY, Zhao SG, et al. Very Early Salvage Radiotherapy Improves Distant Metastasis-Free Survival. The Journal of Urology. 2017;197(3, Part 1):662-8 https://doi.org/10.1016/j.juro.2016.08.106.

88. Trock BJ, Han M, Freedland SJ, Humphreys EB, DeWeese TL, Partin AW, et al. Prostate Cancer–Specific Survival Following Salvage Radiotherapy vs Observation in Men With Biochemical Recurrence After Radical Prostatectomy. JAMA. 2008;299(23):2760-9 https://doi.org/10.1001/jama.299.23.2760.

89. Pfister D, Bolla M, Briganti A, Carroll P, Cozzarini C, Joniau S, et al. Early Salvage Radiotherapy Following Radical Prostatectomy. European Urology. 2014;65(6):1034-43 https://doi.org/10.1016/j.eururo.2013.08.013.

90. Ghadjar P, Hayoz S, Bernhard J, Zwahlen DR, Hölscher T, Gut P, et al. Acute Toxicity and Quality of Life After Dose-Intensified Salvage Radiation Therapy for Biochemically Recurrent Prostate Cancer After Prostatectomy: First Results of the Randomized Trial SAKK 09/10. J Clin Oncol. 2015;33(35):4158-66 https://doi.org/10.1200/jco.2015.63.3529.

91. Shipley WU, Seiferheld W, Lukka HR, Major PP, Heney NM, Grignon DJ, et al. Radiation with or without Antiandrogen Therapy in Recurrent Prostate Cancer. N Engl J Med. 2017;376(5):417-28 https://doi.org/10.1056/NEJMoa1607529.

92. King CR. The Timing of Salvage Radiotherapy After Radical Prostatectomy: A Systematic Review. International Journal of Radiation Oncology*Biology*Physics. 2012;84(1):104-11 https://doi.org/10.1016/j.ijrobp.2011.10.069.

93. Briganti A, Karnes RJ, Joniau S, Boorjian SA, Cozzarini C, Gandaglia G, et al. Prediction of Outcome Following Early Salvage Radiotherapy Among Patients with Biochemical Recurrence After Radical Prostatectomy. European Urology. 2014;66(3):479-86 https://doi.org/10.1016/j.eururo.2013.11.045.

94. Buskirk SJ, Pisansky TM, Schild SE, Macdonald OK, Wehle MJ, Kozelsky TF, et al. Salvage Radiotherapy for Isolated Prostate Specific Antigen Increase After Radical Prostatectomy: Evaluation of Prognostic Factors and Creation of a Prognostic Scoring System. The Journal of Urology. 2006;176(3):985-90 https://doi.org/10.1016/j.juro.2006.04.083.

95. Ward JF, Zincke H, Bergstralh EJ, Slezak JM, Blute ML. PROSTATE SPECIFIC ANTIGEN DOUBLING TIME SUBSEQUENT TO RADICAL PROSTATECTOMY AS A PROGNOSTICATOR OF OUTCOME FOLLOWING SALVAGE RADIOTHERAPY. The Journal of Urology. 2004;172(6, Part 1):2244-8 https://doi.org/10.1097/01.ju.0000145262.34748.2b.
96. Freidlin B, Simon R. Evaluation of randomized discontinuation design. J Clin Oncol. 2005;23(22):5094-8 https://doi.org/10.1200/jco.2005.02.520.
97. Temple RJ. Enrichment Designs: Efficiency in Development of Cancer Treatments. Journal of Clinical Oncology. 2005;23(22):4838-9 https://doi.org/10.1200/jco.2005.02.913.
98. Gunnlaugsson A, Kjellen E, Bratt O, Ahlgren G, Johannesson V, Blom R, et al. PSA decay during salvage radiotherapy for prostate cancer as a predictor of disease outcome - 5 year follow-up of a prospective observational study. Clin Transl Radiat Oncol. 2020;24:23-8 https://doi.org/10.1016/j.ctro.2020.05.008.
99. Cox JD, Stetz J, Pajak TF. Toxicity criteria of the Radiation Therapy Oncology Group (RTOG) and the European organization for research and treatment of cancer (EORTC). International Journal of Radiation Oncology*Biology*Physics. 1995;31(5):1341-6 https://doi.org/10.1016/0360-3016(95)00060-C.
100. Aaronson NK, Ahmedzai S, Bergman B, Bullinger M, Cull A, Duez NJ, et al. The European Organization for Research and Treatment of Cancer QLQ-C30: a quality-of-life instrument for use in international clinical trials in oncology. J Natl Cancer Inst. 1993;85(5):365-76 https://doi.org/10.1093/jnci/85.5.365.
101. van Andel G, Bottomley A, Fosså SD, Efficace F, Coens C, Guerif S, et al. An international field study of the EORTC QLQ-PR25: a questionnaire for assessing the health-related quality of life of patients with prostate cancer. Eur J Cancer. 2008;44(16):2418-24 https://doi.org/10.1016/j.ejca.2008.07.030.
102. Feygelman V, Stambaugh C, Zhang G, Hunt D, Opp D, Wolf TK, et al. Motion as a perturbation: Measurement-guided dose estimates to moving patient voxels during modulated arc deliveries. Medical Physics. 2013;40(2):021708 https://doi.org/10.1118/1.4773887.
103. Gay HA, Barthold HJ, O'Meara E, Bosch WR, El Naqa I, Al-Lozi R, et al. Pelvic normal tissue contouring guidelines for radiation therapy: a Radiation Therapy Oncology Group consensus panel atlas. Int J Radiat Oncol Biol Phys. 2012;83(3):e353-62 https://doi.org/10.1016/j.ijrobp.2012.01.023.
104. Brock KK, Mutic S, McNutt TR, Li H, Kessler ML. Use of image registration and fusion algorithms and techniques in radiotherapy: Report of the AAPM Radiation Therapy Committee Task Group No. 132. Med Phys. 2017;44(7):e43-e76 https://doi.org/10.1002/mp.12256.
105. Churruca K, Pomare C, Ellis LA, Long JC, Henderson SB, Murphy LED, et al. Patient-reported outcome measures (PROMs): A review of generic and condition-specific measures and a discussion of trends and issues. Health Expect. 2021;24(4):1015-24 https://doi.org/10.1111/hex.13254.

106. Zaniletti I, Gunn HJ, Hallemeier CL, Laughlin BS, Leavitt TR, Haddock MG, et al. Determining the Minimal Clinically Important Difference of the FACT-Hep to Evaluate the Change in the Quality of Life (QOL) of Pancreatic Cancer (PC) Patients During Radiotherapy. Int J Radiat Oncol Biol Phys. 2023 https://doi.org/10.1016/j.ijrobp.2023.08.009.
107. Kestin L, Goldstein N, Vicini F, Yan D, Korman H, Martinez A. Treatment of prostate cancer with radiotherapy: should the entire seminal vesicles be included in the clinical target volume? Int J Radiat Oncol Biol Phys. 2002;54(3):686-97 https://doi.org/10.1016/s0360-3016(02)03011-0.
108. Duan X, Chen L, Zhou Y. Evaluation of target autocrop function in nasopharyngeal carcinoma SIB IMRT plan. Phys Eng Sci Med. 2022;45(1):97-105 https://doi.org/10.1007/s13246-021-01082-3.
109. Viswanathan AN, Yorke ED, Marks LB, Eifel PJ, Shipley WU. Radiation dose-volume effects of the urinary bladder. Int J Radiat Oncol Biol Phys. 2010;76(3 Suppl):S116-22 https://doi.org/10.1016/j.ijrobp.2009.02.090.
110. Michalski JM, Gay H, Jackson A, Tucker SL, Deasy JO. Radiation Dose–Volume Effects in Radiation-Induced Rectal Injury. International Journal of Radiation Oncology*Biology*Physics. 2010;76(3, Supplement):S123-S9 https://doi.org/10.1016/j.ijrobp.2009.03.078.
111. Lu JY, Lin Z, Zheng J, Lin PX, Cheung ML, Huang BT. Dosimetric evaluation of a simple planning method for improving intensity-modulated radiotherapy for stage III lung cancer. Sci Rep. 2016;6:23543 https://doi.org/10.1038/srep23543.
112. Amaloo C, Nazareth DP, Kumaraswamy LK. Comparison of hybrid volumetric modulated arc therapy (VMAT) technique and double arc VMAT technique in the treatment of prostate cancer. Radiol Oncol. 2015;49(3):291-8 https://doi.org/10.1515/raon-2015-0018.
113. Terlizzi M, Bossi A. Re: The Addition of Androgen Deprivation Therapy and Pelvic Lymph Node Treatment to Prostate Bed Salvage Radiotherapy (NRG Oncology/RTOG 0534 SPPORT): An International, Multicentre, Randomised Phase 3 Trial. Eur Urol. 2023;83(5):475 https://doi.org/10.1016/j.eururo.2022.12.026.
114. Landry G, Kurz C, Traverso A. The role of artificial intelligence in radiotherapy clinical practice. BJR Open. 2023;5(1):20230030 https://doi.org/10.1259/bjro.20230030.
115. Mylona E, Acosta O, Lizee T, Lafond C, Crehange G, Magné N, et al. Voxel-Based Analysis for Identification of Urethrovesical Subregions Predicting Urinary Toxicity After Prostate Cancer Radiation Therapy. Int J Radiat Oncol Biol Phys. 2019;104(2):343-54 https://doi.org/10.1016/j.ijrobp.2019.01.088.
116. Mireștean CC, Iancu RI, Iancu DPT. Simultaneous Integrated Boost (SIB) vs. Sequential Boost in Head and Neck Cancer (HNC) Radiotherapy: A Radiomics-Based Decision Proof of Concept. J Clin Med. 2023;12(6) https://doi.org/10.3390/jcm12062413.

117. Franco P, De Bari B, Arcadipane F, Lepinoy A, Ceccarelli M, Furfaro G, et al. Comparing simultaneous integrated boost vs sequential boost in anal cancer patients: results of a retrospective observational study. Radiation Oncology. 2018;13(1):172 https://doi.org/10.1186/s13014-018-1124-9.
118. Songthong AP, Kannarunimit D, Chakkabat C, Lertbutsayanukul C. A randomized phase II/III study of adverse events between sequential (SEQ) versus simultaneous integrated boost (SIB) intensity modulated radiation therapy (IMRT) in nasopharyngeal carcinoma; preliminary result on acute adverse events. Radiation Oncology. 2015;10(1):166 https://doi.org/10.1186/s13014-015-0472-y.
119. Kahvecioglu A, Gurlek E, Yedekci FY, Sari SY, Gultekin M, Yildiz F. Simultaneous integrated or sequential boost to clinically involved lymph nodes in patients with locally advanced cervical cancer treated with definitive chemoradiotherapy. Gynecol Oncol. 2023;176:10-5 https://doi.org/10.1016/j.ygyno.2023.06.020.
120. Zheng D, Hong JC, Wang C, Zhu X. Radiotherapy Treatment Planning in the Age of AI: Are We Ready Yet? Technol Cancer Res Treat. 2019;18:1533033819894577 https://doi.org/10.1177/1533033819894577.

Appendix

The following appendix describes the adaptive sequential plan-on-plan VMAT radiotherapy treatment planning method used for all patients included in the PROPER 1 trial. The Eclipse planning system, version 15.6 (Varian Medical Systems, Palo Alto, CA, USA) [3] was used for treatment planning.

Description of the adaptive sequential plan-on-plan VMAT radiotherapy treatment planning in the PROPER 1 study.

Prescription

- All patients are initially prescribed 70.0 Gy/35 fractions to the prostate bed, treatment plan 1.
- Treatment prediction is performed after 25 fractions.
- Treatment responders (PSA < 15 ng/mL 5w) continue SRT to 70.0 Gy/35 fractions according to prescription (treatment plan 1).
- Treatment non-responders (PSA ≥ 15 ng/mL 5w) are additionally prescribed 50.0 Gy to the pelvic lymph nodes:
  - Treatment plan 2: prostate bed + pelvic lymph nodes, 20 Gy/10 fractions.
  - Treatment plan 3: pelvic lymph nodes, 30 Gy/15 fractions.

Treatment plan 1, the prostate bed (PTV-P) 70.0 Gy/35 fr.

a) Following the target, help structures were created (if local boost).
   i) X_PTV-P: PTV-P excluding PTV-T with 5 mm margin.

b) Following OAR, help structures were created. (Figure I).
   i) Z_Bladder: Bladder excluding PTV-P with 5 mm margin.
   ii) Z_Rectum: Rectum with isotropic 5 mm margin excluding PTV-P with 5 mm margin.
   iii) Z_Rectum AND PTV: the overlapping region between rectum and PTV-P.

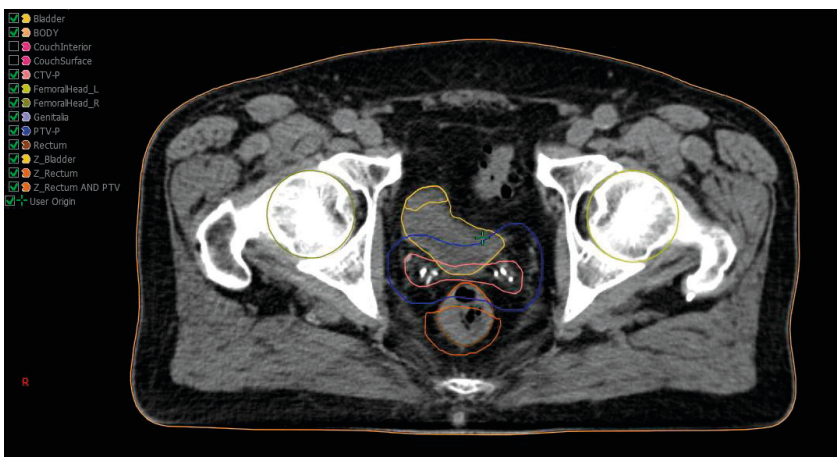

Figure I

c) Creation of treatment plan 1.
   i) Target volume PTV-P.
   ii) Recommended energy, 10 MV.
   iii) Two arcs with a collimator angle of 5 deg. Full rotation is recommended for homogeneous dose distribution, which is essential due to the dose in the inter-phase junction in the case of PLNRT.
   iv) Use the Arc Geometry Tool to align fields to PTV-P.
   v) Target Margin 5 mm.
   vi) Place the isocentre (cranial/caudal direction) in the most cranial slice of PTV-P to use the same isocenter in all plans in case of PLNRT.
   vii) If the function Fine-tune Fields is used. Let Fine-tune Fields set the collimator again (after the isocenter moves to the cranial slice) without adjusting the isocenter.

d) Optimization.
   i) Use the objective values from Figure IIa. Use these values as the starting parameters. Note that the priority for all OAR is set to 0.
   ii) In case of boost volume, insert values from Figure IIb.
   iii) Set Normal Tissue Objective (NTO) according to Figure IIa/b.
   iv) MU Objective should be less than 600 MU to reduce the plan complexity.
   v) Automatic Optimization Mode and Automatic Intermediate Dose should be used.
   vi) Start the optimiser, let it go to MR Level 1 and Step 4 and pause the optimisation.
   vii) Optimize objectives for the OAR to suit the current patient and set the priority value on each objective.
   viii) Set Priority to 150-160 on high-priority OAR, in this case Z_Rectum and Z_Bladder, and 120-130 on lower-priority risk organs, Genitalia and FemoralHead_L and FemoralHead_R.
   ix) Z_Rectum AND PTV with Priority 180-200 is used to avoid hot spots in the rectum.
   x) Start the optimisation again. Follow the optimisation and keep track of all objectives that "work" appropriately; PTV and NTO have the highest priority, but all OARs are working relatively well!
   xi) Normalize the plan to the median dose after the final dose calculation.
   xii) Check that all target and OAR objectives are met; see Table 1.
   xiii) The 3-4 most cranial slices in PTV-P are the area that will be in the inter-phase junction in the case of PLNRT. Therefore, having $D_{max} < 103\%$ in these slices is essential. In case of doses over 103% in this area, it is recommended to create the structure of, e.g., 102% doses and use it to optimise down the D_{max}.
   xiv) If all requirements are unmet, or the dose in most cranial slices is too high, start the optimiser again and continue the previous optimisation. Reverse one or more MR Levels depending on how large changes are needed to create an optimal plan.

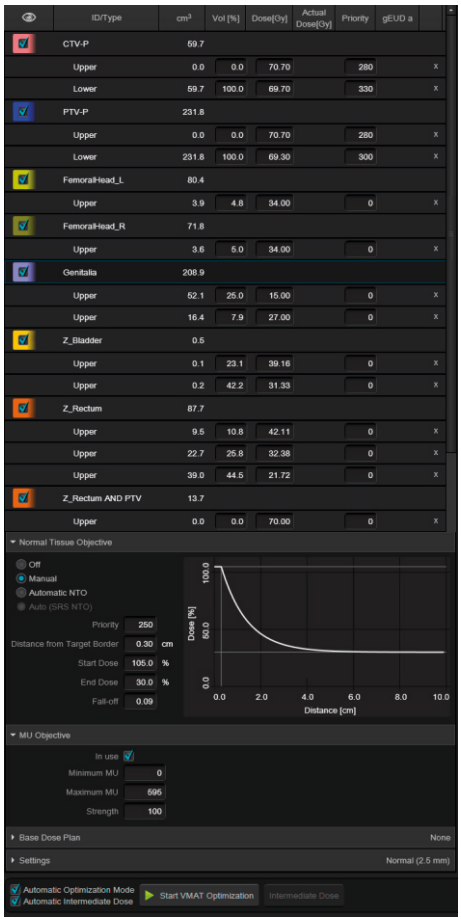

Figure IIa

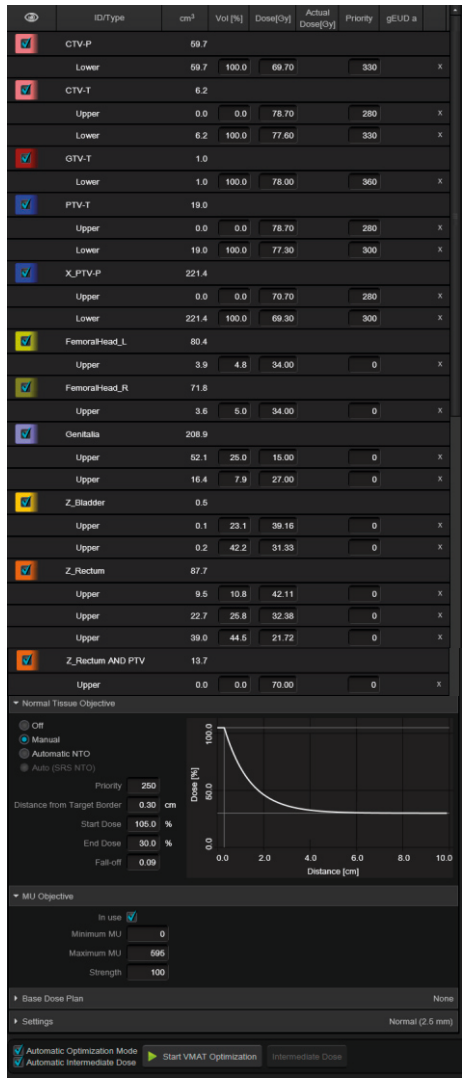

Figure IIb

Treatment plan 2, the prostate bed (PTV-P) and the pelvic lymph nodes (PTV-N) 20.0 Gy/10fr.

a) Create the following target help structures (Figure III)
   i) X_(50-70)+(0-20): The sum of PTV-P and PTV-N_50.0.
   ii) If boost, exclude PTV-T or/and PTV-Lmet from X_(50-70)+(0-20) with a 5mm margin.

b) Create the following OAR help structures (Figure III)
   i) Z_Bladder1: Bladder excluding X_(50-70)+(0-20)with 5mm margin.
   ii) Z_Rectum1: Rectum with isotropic 5mm margin excluding X_(50-70)+(0-20) with 5mm margin.
   iii) Z_Rectum AND PTV1: overlapping region between Rectum and X_(50-70)+(0-20).
   iv) Z_BowelBag: Y_BowelBag[-5mm] excluding X_(50-70)+(0-20) with 15mm margin.

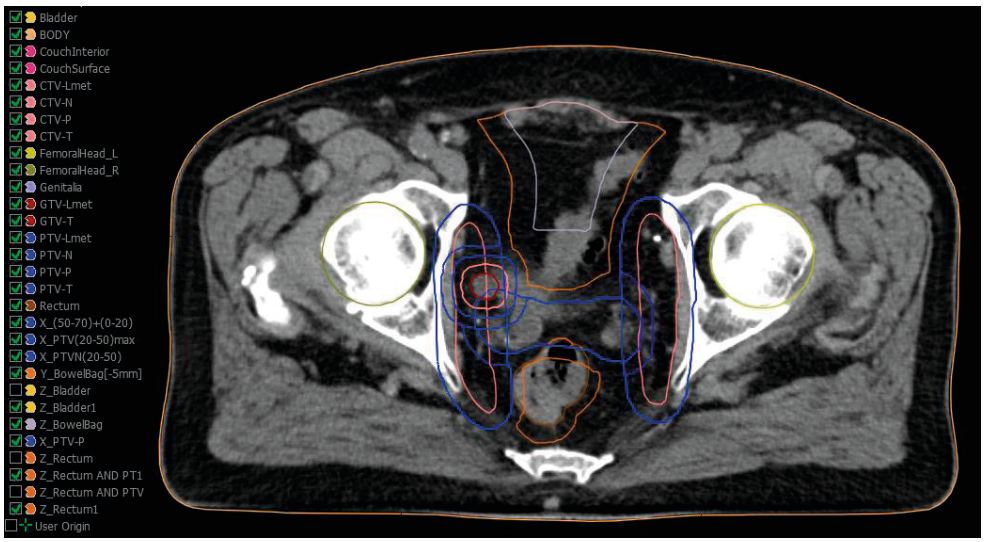

Figure III

c) Creation of treatment plan 2.
   i) Target volume X_(50-70)+(0-20).
   ii) Recommended energy is 10 MV.
   iii) Use the same isocenter coordinates as in treatment plan 1.
   iv) Two arcs with a collimator angle of 5 deg. and full rotations.
   v) Use the Arc Geometry Tool to align fields to X_(50-70)+(0-20).
   vi) Target Margin 0.5cm. (Figure IV)

vii) To achieve high dose conformity for the target volumes and to spare the OAR, a maximum field size of about 15 cm in the MLC direction could be used due to the limitations of the MLC movements (Varian). Decrease X1 for arc one to obtain a maximum field size of 15 cm, and vice versa for X2 in arc two (X1/X2 according to IEC61217) (Figure V).

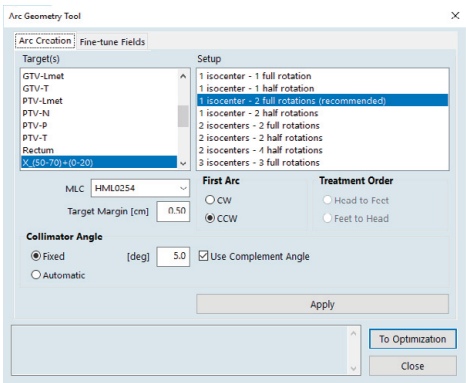

Figure IV

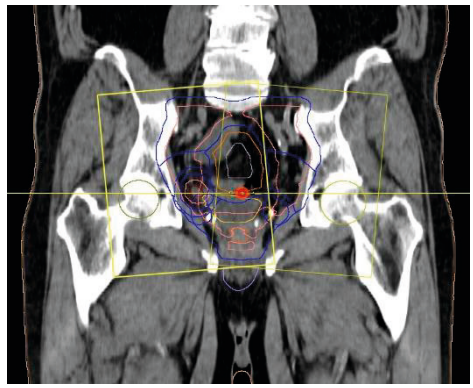

Figure V

d) Optimization
   i) Use the objective values from Figure VIa. Use these values as the starting parameters. Note that the priority for all OAR is set to 0.
   ii) In case of boost volume, insert values from Figure VIb.
   iii) Set Normal Tissue Objective according to Figure VIa/b.
   iv) MU Objective should be set to less than 1100 MU to reduce the plan complexity.
   v) Automatic Optimization Mode and Automatic Intermediate Dose should be used.
   vi) Start the optimiser, let it go to MR Level 1 and Step 4, and pause the optimisation.
   vii) Optimize objectives for the OAR to suit the current patient and set the priority value on each objective.
   viii) Set Priority to 150-160 on high-priority OAR, in this case, Y_BowelBag[-5mm], Z_BowelBag, Z_Rectum1 and Z_Bladder1, and 120-130 on lower-priority OAR, Genitalia and FemoralHeads_L and FemoralHead_R.
   ix) Z_Rectum AND PT1 with Priority 180-200 is used to avoid hot spots in the rectum.
   x) Start the optimisation again. Follow the optimisation and track that all objectives "work" appropriately; PTV and NTO have the highest priority, but all OAR are working relatively!
   xi) Normalize the plan to the median dose after the final dose calculation.
   xii) Evaluation of OAR can not be done until all three plans are ready and a plan summation can be done.

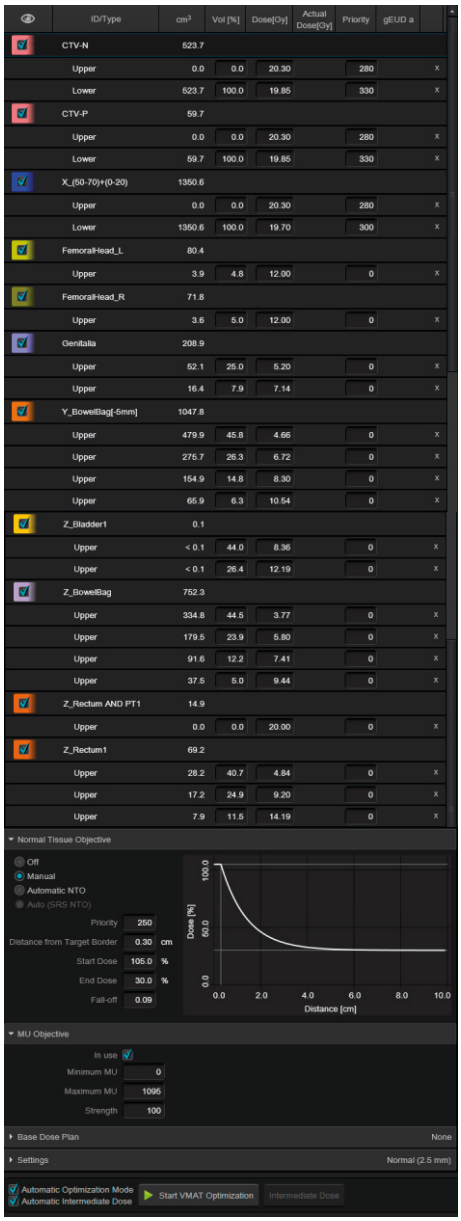

Figure VIa

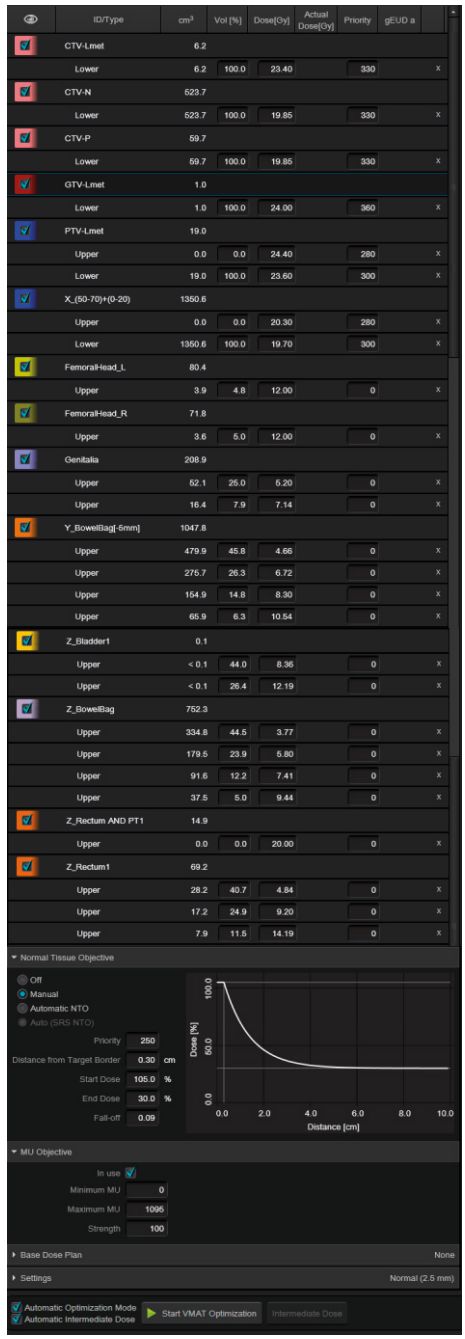

Figure VIb

Treatment plan 3, the pelvic lymph nodes (PTV-N) 30.0 Gy/15fr.

a) Make a copy of plan one and change the fractionation to 50.0Gy/25fr. Ensure that the MU per field is preserved and that only the number of fractions and total dose are changed. Name the copy with the suffix 50.0Gy. This copy will be used for the sum of all three plans in the case of PLNRT.

b) Make an $EQD2_{\alpha/\beta=3}$ correction of the 50.0Gy plan copy. Name the plan with the prefix EQD2. This EQD2 corrected plan will be used as a base plan in the optimisation of plan 3.

c) Create the following target help structure.
   i) X_PTV-N(20-50): PTV-N_50.0 excluding PTV-P with 5 mm margin.
   ii) X_PTV-N(20-50)max: PTV-N_50.0 excluding PTV-P with 30 mm margin.
   iii) If boost , exclude PTV-Lmet from X_PTV-N(20-50) and X_PTV-N(20-50)max with a 5mm margin.

d) The same OAR help structures are used for treatment plan 2.

e) Creation of treatment plan 3.
   i) Target volume X_PTV-N(20-50).
   ii) Recommended energy is 10 MV.
   iii) Use the same isocenter coordinates as in treatment plan 1.
   iv) Two arcs with a collimator angle of 5 deg. and full rotations.
   v) Use the Arc Geometry Tool to align fields to X_PTV-N(20-50).
   vi) Target Margin 5 mm.
   vii) To achieve high dose conformity for the target volumes and to spare the OAR, a maximum field size of about 15 cm in the MLC direction could be used due to the limitations of the MLC movements (Varian). Decrease X1 for arc one to obtain a maximum field size of 15 cm, and vice versa for X2 in arc two (X1/X2 according to IEC61217). Figure V.

f) Optimization
   i) Use the objective values from Figure VIIa. Use these values as the starting parameters. Note that the priority for all OAR is set to 0.
   ii) In case of boost volume, insert values from Figure VIIb.
   iii) Note that PTV-P is used with the Upper objective of limiting the dose to the prostate bed during optimisation. And a Lower objective with Priority 0 for better functionality of the Normal Tissue Objective.
   iv) Set Normal Tissue Objective according to Figure VIIa/b.
   v) Use the EQD2 corrected plan 1 with 50Gy/25fr as Base Dose Plan (Fig.VII).
   vi) MU Objective should be set to less than 1100 MU to reduce the plan complexity.

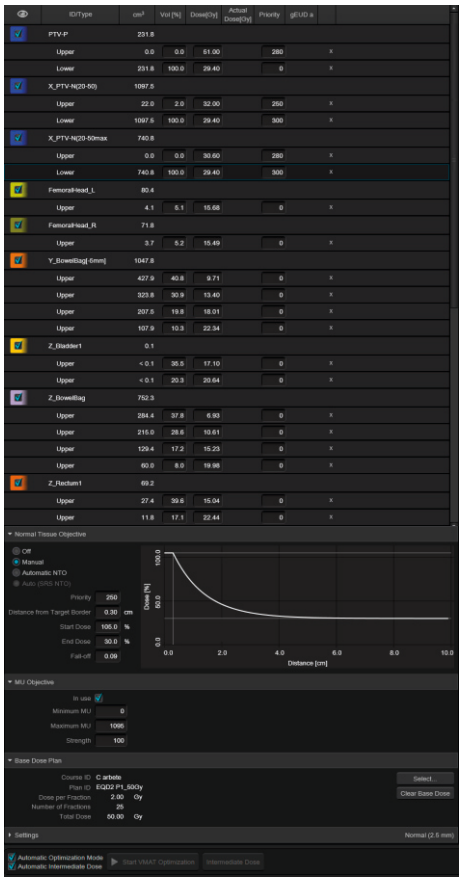

Figure VIIa

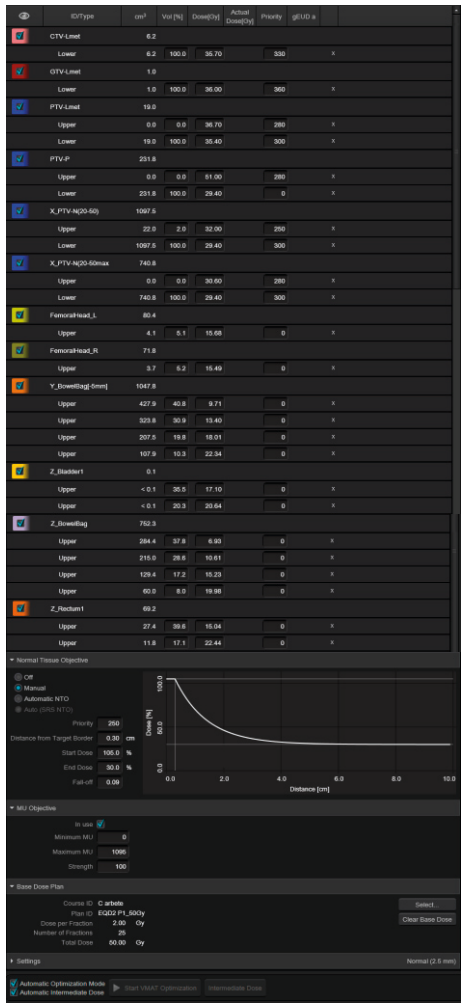

Figure VIIb

vii) Automatic Optimization Mode and Automatic Intermediate Dose should be used.

viii) Start the optimiser, let it go to MR Level 1 and Step 4, and pause the optimisation.

ix) Move all objectives for the OAR to suit the current patient and set the priority value on each objective.

x) Set Priority to 150-160 on high-priority OAR, in this case, Y_BowelBag[-5mm], Z_BowelBag, Z_Rectum1 and Z_Bladder1 and 120-130 on lower-priority OAR, FemoralHeads_L and FemoralHead_R.

xi) Start the optimisation again. Follow the optimisation and track that all objectives "work" appropriately; PTV and NTO have the highest priority, but all OAR are working relatively!

xii) After dose calculation, the plan should generally not be normalised. Due to the dose fall off in the inter-phase junction, it does not fit to normalise the plan to the median dose.

g) Plan evaluation

i) Make a plan summation including treatment plan 1 (copy of plan 50Gy/25 fr), plan two and plan 3 (Figure VIII). Check all dose criteria according to Table I.

ii) Make an $EQD2_{\alpha/\beta = 3}$ Gy plan summation, including all treatment plans (Figure IX). Check dose criteria for CTV-N_50.0 and PTV-N_50.0 according to Table 1.

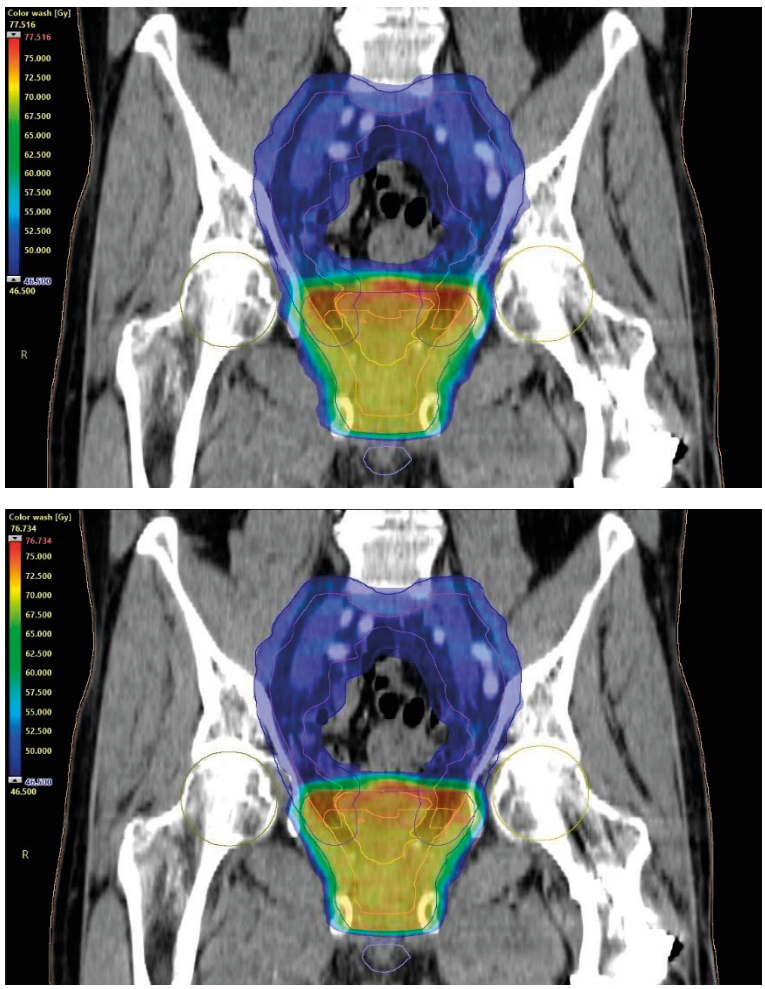

Figure VIII

Plan summation in $EQD2_{\alpha/\beta = 3}$ corrected dose.

Priority	VOI	Prescribed dose (dose/fraction)	Dose/volume recommendation
1	GTV-T	78.0 Gy (2.0+ Gy)	$D_{99\%} \geq 76.0$ Gy
2	CTV-T	78.0 Gy (2.0+ Gy)	$D_{98\%} \geq 76.0$ Gy
3	PTV-T	78.0 Gy (2.0+ Gy)	$D_{98\%} \geq 74.0$ Gy
4	CTV-P	70.0 Gy (2.0 Gy)	$D_{99\%} \geq 68.0$ Gy
5	PTV-P	70.0 Gy (2.0 Gy)	$D_{98\%} \geq 66.0$ Gy
6	GTV-Lmet	60.0 Gy (2.4 Gy)	$D_{99\%} \geq 58.0$ Gy
7	CTV-Lmet	60.0 Gy (2.4 Gy)	$D_{98\%} \geq 58.0$ Gy
8	PTV-Lmet	60.0 Gy (2.4 Gy)	$D_{98\%} \geq 57.0$ Gy
9	Fixed bowel loop		$V_{50Gy} < 17$ cm^3
			$D_{2\%} \leq 60.0$ Gy
10	Rectum		$V_{70Gy} < 20$ %
11	CTV-N	50.0 Gy (2.0 Gy)	$D_{99\%} \geq 47.5$ Gy
12	Rectum		$V_{75Gy} < 15$ %
13	PTV-N	50.0 Gy (2.0 Gy)	$D_{99\%} \geq 46.5$ Gy
14	Femoral heads		$D_{max} \leq 55.0$ Gy
15	BowelBag - PTV5mm		$V_{30Gy} < 300$ cm^3
			$V_{40Gy} < 150$ cm^3
			$V_{45Gy} < 100$ cm^3
			$V_{50Gy} < 35$ cm^3
16	Rectum		$V_{60Gy} < 35$ %
17	BODY		$D_{max} \leq 82.0$ Gy
18	Bladder		$D_{medel} \leq 62.0$ Gy

Table I

Dose-volume objectives (physical dose).